Advances in Polymer Technology

Antifouling Polymer Technology for Healthcare Applications

Lead Guest Editor: Nasir M. Ahmad
Guest Editors: Shenmin Zhu, Hazim Qiblawey, and Abdelhamid Elaissari

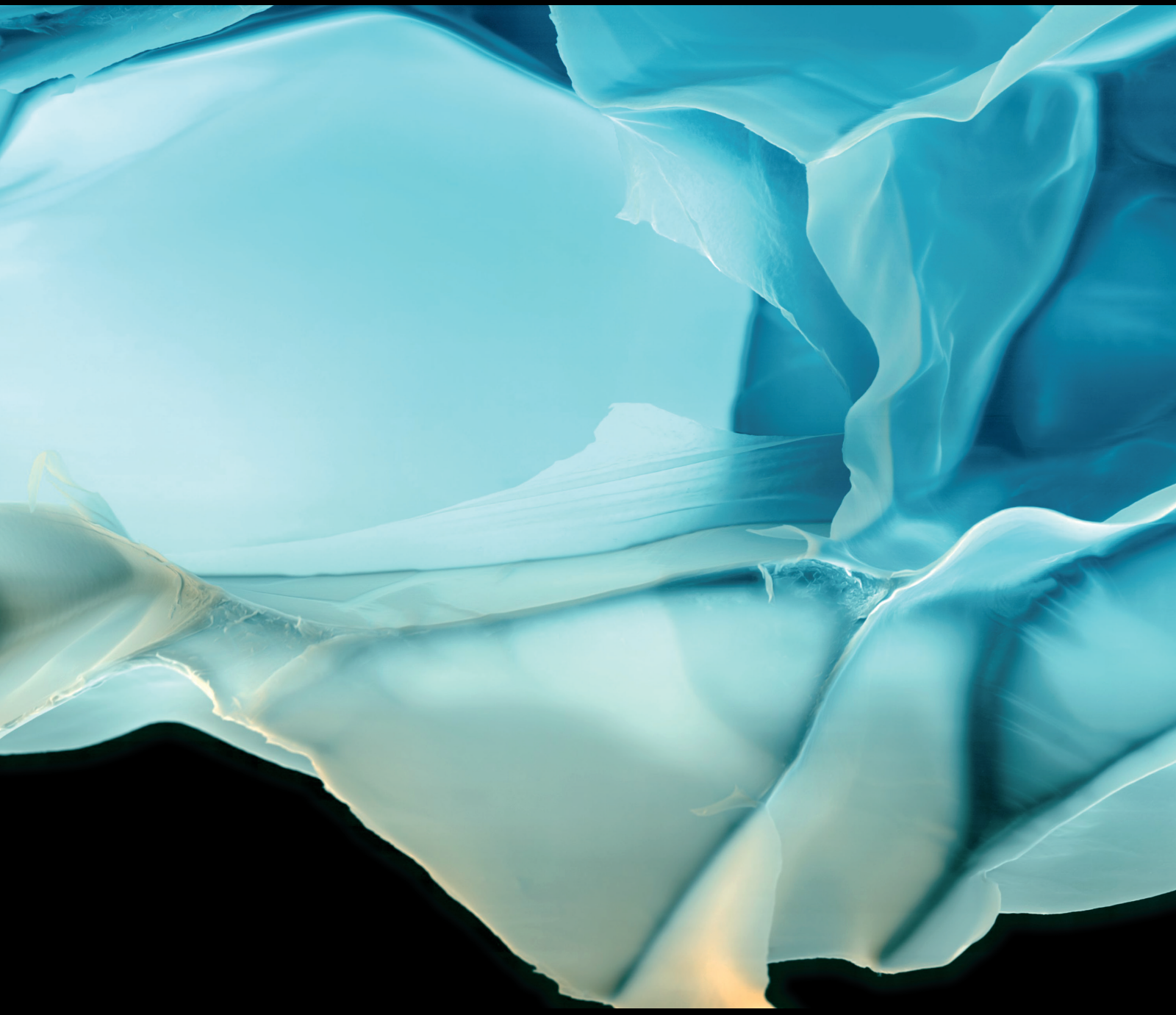

Antifouling Polymer Technology for Healthcare Applications

Advances in Polymer Technology

Antifouling Polymer Technology for Healthcare Applications

Lead Guest Editor: Nasir M. Ahmad
Guest Editors: Shenmin Zhu, Hazim Qiblawey, and Abdelhamid Elaissari

Contents

Hindawi
Advances in Polymer Technology
Volume 2021, Article ID 6627736, 9 pages
https://doi.org/10.1155/2021/6627736

Research Article

Antialgal Synergistic Polystyrene Blended with Polyethylene Glycol and Silver Sulfadiazine for Healthcare Applications

M. Raheel Anjum,[1] Shehla Mushtaq,[2] M. Asad Abbas,[1] Azhar Mahmood,[2] Habib Nasir,[2] Hussnain A. Janjua,[3] Qamar Malik,[4] and Nasir M. Ahmad[1]

[1]*Polymer Research Lab, School of Chemical and Material Engineering (SCME), National University of Sciences and Technology (NUST), Sector H-12, Islamabad 44000, Pakistan*
[2]*Department of Chemistry, School of Natural Sciences (SNS), NUST, Sector H-12, Islamabad 44000, Pakistan*
[3]*Department of Industrial Biotechnology, Atta-Ur-Rahman School of Applied Biosciences (ASAB), NUST, Sector H-12, Islamabad 44000, Pakistan*
[4]*ABBOTT Energy & Environment Inc., Alastair Ross Technology Centre, 3553 31st Street NW, Calgary, AB, Canada T2L 2A6*

Correspondence should be addressed to Nasir M. Ahmad; nasir.ahmad@scme.nust.edu.pk

Received 21 October 2020; Revised 3 October 2021; Accepted 22 October 2021; Published 25 November 2021

Academic Editor: Kinga Pielichowska

Polystyrene (PS) was blended with polyethylene glycol (PEG) and silver sulfadiazine (SS) with different weight proportions to form polymeric blends. These synthesized blends were preliminary characterized in terms of functional groups through the FTIR technique. All compositions were subjected to thermogravimetric analysis for studying thermal transition and were founded thermally stable even at 280°C. The zeta potential and average diameter of algal strains of *Dictyosphaerium* sp. (DHM1), *Dictyosphaerium* sp. (DHM2), and *Pectinodesmus* sp. (PHM3) were measured to be -32.7 mV, -33.0 mV, and -25.7 mV and 179.6 nm, 102.6 nm, and 70.4 nm, respectively. Upon incorporation of PEG and SS into PS blends, contact angles were decreased while hydrophilicity and surface energy were increased. However, increase of surface energy did not led to decrease of antialgal activities. This has indicated that biofilm adhesion is not a major antialgal factor in these blended materials. The synergetic effect of PEG and SS in PS blends has exhibited significant antialgal activity via the agar disk diffusion method. The PSPS10 composition with 10 *w*/*w*% PEG and 10 *w*/*w*% SS has exhibited highest inhibition zones 10.8 mm, 10.8 mm, and 11.3 mm against algal strains DHM1, DHM2, and DHM3, respectively. This thermally stable polystyrene blends with improved antialgal properties have potential for a wide range of applications including marine coatings.

1. Introduction

Biofouling is an undesired build-up of biotic deposits on a material's surface. This biotic deposit includes different species such as cyanobacteria, algal spores, fungi, and macroalgae [1]. Biofouling thus may be either microbial based or combination of micro- and macroattack caused by the synergetic effect of microbial and macroorganism, respectively [2]. Algal biofouling is a specific type of biodegradation initiated by algae in highly humid as well as aquatic environment and multiplies in their numbers that lead to attachment of other biological species spiraling it into complex heterogeneous system of macrobiofouling [1]. The biological degradation of certain material depends specifically on the type of microorganisms, environmental conditions, and its physical and chemical properties [3]. Microbial growth adversely affects numerous areas relevant to food preservation, water purification, photobioreactors, bioimplants, and biosensors in healthcare applications [4]. Microbial growth can be inhibited by different types of materials like nanocomposite, polymer composites, and polymeric systems [5]. Among these materials, polymer-based systems are the best antimicrobial materials and have numerous advantages over conventional materials with exceptional film-forming ability, suitable chemical activity, thermal stability, mechanical strength, corrosion resistance, and low cost [6]. Various antifouling

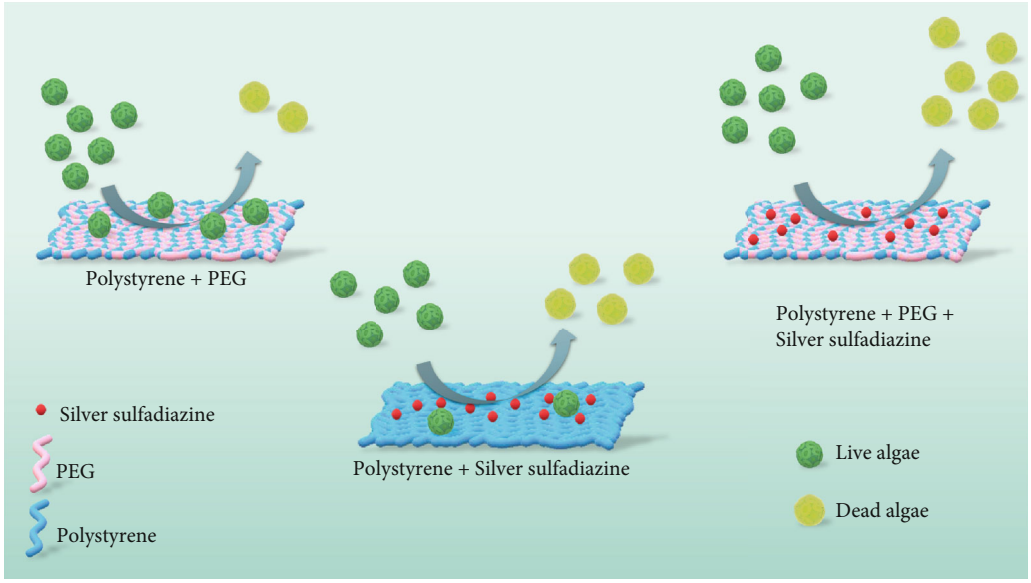

Figure 1: Schematic of various blends showing antialgal properties.

polymer systems were developed to exhibit increased efficiency, enhanced antimicrobial behavior, process ability, tunable properties, low toxicity, prolonged life time, and diverse functionalities [7, 8]. Therefore, antifouling polymer-based systems have given an innovative direction to the research in the field of antimicrobial materials. Surface features like hydrophilicity, surface roughness, polarity, surface energy, and contact angle are important parameters to design antifouling systems [9]. Polymer-based antifouling blends are used in a wide variety of forms including copolymers, grafting, polymer coatings, thin films, polymer brushes, and polyelectrolytes [10].

Gitchaiwat et al. have enhanced antialgal property of LDPE against the *Chlorella vulgaris* TISTR 8580 species by adding the antialgal agent such as 2-methylthio-4-ethylamino-6-tert-butylamino-triazin-1,3,5 [terbutryn (TT)] [11]. The results have shown that TT with an optimal loading of 750 ppm could be used to effectively inhibit the growth of *C. vulgaris*, but to get satisfactory inhabitation iodopropynyl butylcarbamate (IPBC) could be used as antialgal promoters in the LLDPE specimens [11]. In another study, Yandi and coworkers have investigated the antialgal activity of cationic poly(2-(dimethylamino)ethyl methacrylate) (PDMAEMA) brushes against marine algae *Ulva linza* and *U. lactuca* [12]. PDMAEMA has been found to destroy zoospores in contact with it and also avoid the subsequent development of normally settled spores [12]. Bodkhe et al. have used PSBMA as part of a block copolymer with PDMS that was incorporated into the polyurethane network. Although these coatings had excellent fouling resistance properties against the marine bacterium *Halomonas pacifica* and *N. incerta*, the performance was less pronounced against algal species *Cellulophaga lytica* and *U. linza* [13]. In a recent study, 3-sulfopropylmethacrylate was copolymerized with methyl methacrylate that only controls the adhesion of *Dictyosphaerium* algae but did not kill the algal cells [14]. These literature studies have indicated that the most polymeric systems could significantly inhibit bacterial species but could not be used effectively against algal species. To overcome this discrepancy, hydrophilic polymers such as PEG could be introduced to the polymeric system [15]. PEG due to polar nature and strong hydrogen bonding leads to excluded volume which makes the adsorption of fouling organisms extremely difficult on its surface [16]. PEG-based antifouling system acts as a biopassive material which effectively reduces the microbial adhesion owing to the formation of an interfacial layer [17]. The PEG moieties present on various frictional surfaces have shown strong resistance towards nonspecific proteins and cell adsorption. This minimizes the amount of bioadhesion on these surfaces and makes PEG highly desirable for antifouling purposes [17, 18].

In the current novel work, blending of polystyrene (PS), polyethylene glycol (PEG), and silver sulfadiazine was carried out by varying the concentration of constituents via the melt-blending technique. Blend synthesis was confirmed through FTIR, and thermal stability was studied through TGA. The equilibrium contact angle of various compositions was measured, and the surface energy of compositions was calculated with the help of contact angle. The antialgal assay of all blends was performed against three different algal strains *Dictyosphaerium* sp. (DHM1), *Dictyosphaerium* sp. (DHM2), and *Pectinodesmus sp.* (PHM3) by the agar disk diffusion method via zone of inhibition measurement. The PSPS10 blend has demonstrated a maximum zone of inhibition against these algal strains. Figure 1 shows the antialgal behavior of the various blends indicating PSPS10 has the maximum antialgal efficiency.

2. Experimental

2.1. Materials. All the chemical and reagent are of analytical grade. Polyethylene glycol (Mw-1000, 99.99%) was purchased from Daejung Chemicals, S. Korea, Polystyrene (Melt flow index 2-4 g/10 min; Mw-350000, 95%, average

Table 1: Compositions of blends.

Sample code	PS w/w%	PEG w/w%	SS w/w%
PS	100	0	—
PSP5	95	5	—
PSP10	90	10	—
PSP15	85	15	—
PSP20	80	20	—
PSS10	90	—	10
PSPS10	80	10	10

Mn~170,000, density 1.04 g/cm3), and silver sulfadiazine (98%) was purchased from Sigma Aldrich, Germany. Mueller Hinton Agarose was purchased from Merck, UK. Standard algal strains *Dictyosphaerium* sp. (DHM1), *Dictyosphaerium* sp. (DHM2), and *Pectinodesmus sp.* (PHM3) were used as testing species.

2.2. Preparation of Blends. The melt-mixing technique was used for the preparation blends of polystyrene (PS) with polyethylene glycol (PEG), and silver sulfadiazine (SS) was prepared using the internal batch mixer of HAAKE Rheomix model Lab OS by Thermo Fisher Scientific, USA. PEG and SS were utilized as received while PS was meshed to fine powder prior to blend preparation. The temperature of the equipment was raised up to 200°C and held for five minutes to become stabilized on attaining the desired temperature. Afterward, the predetermined composition of blends was fed into the melt mixer, and its mixing was controlled by optimizing parameters such as RPM, temperature, and time. After completion of blending, the blends were retrieved and further molded into sheets of 1 mm thickness by using laboratory press by Gibitre Instrument, Italy. The prepared sheets were finally cold pressed using 30-ton hydraulic press. Table 1 shows blend composition that were made by varying the amount of PEG from 0 to 20% (w/w) and SS from 0 to 10% (w/w).

2.3. Characterization. Infrared spectroscopy (ATR-FTIR) was performed by Bruker's model Alpha-P (USA) for identification of functional groups in various blend compositions. Thermal degradation analysis was performed using TGA model LF2 (Mettler Toledo, USA) equipped with high-temperature furnace in nitrogen atmosphere at the heating rate of 20°C/min. The contact angle of blends was measured by using 5 μL sessile drop of deionized water via a lab-made customized apparatus. The contact angle was measured for each composition by average three values of drops after 2 min with the help of ImageJ software. Since the surface energy of the substrate is based on the contact angle measurement of blends, therefore, the surface energy was calculated by the Chibowski equation [14].

$$\gamma s = \frac{\gamma l}{2}\left(1 + \cos\theta_{Eq}\right). \quad (1)$$

Here, γs is the solid surface energy, γl is the surface energy of liquid, and θ_{Eq} is water equilibrium contact angle.

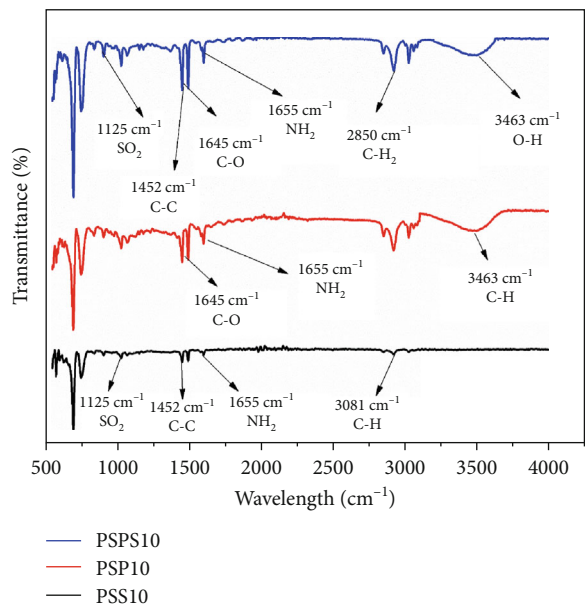

Figure 2: FTIR spectra of PSPS10, PSP10, and PSS10.

The zeta potential and zeta size of algal strains *Dictyosphaerium* sp. (DHM1), *Dictyosphaerium* sp. (DHM2), and *Pectinodesmus* sp. (PHM3) were measured using the Zetasizer model Nano Zsp by Malvern Instruments, UK. Prior to zeta potential measurement, cultures were kept undisturbed for almost 10 minutes to let any flocks settle down, and strains were sampled from the top to be used in experiment.

2.3.1. Antialgal Bioassay. The antialgal profile of various polymeric blends was tested against three different algal strains namely *Dictyosphaerium* sp. (DHM1), *Dictyosphaerium* sp. (DHM2), and *Pectinodesmus* sp. (PHM3). The process commenced with the preparation of algal cell suspension in BBM medium with the initial concentration of 5-7 billion cells per millimeter. The antialgal effect of various samples was studied on the Mueller Hinton Agarose plates inoculated with algal cultures. The agarose solution (1% w/v) of distilled water and bold basal medium (BBM) (4 : 1 by volume, respectively) was prepared [19]. The pouring of plates with agar and spreading of algae onto these agar plates was performed in the safety cabinet that was previously sterilized through UV light (10 to 15 minutes) and cleaned with absolute ethanol. The whole process was performed in sterile conditions close to the spirit lamp to avoid any undesired microbial growth except microalgae. Disks of 6 mm of all samples were placed on agar, and the plates were incubated for 3 to 4 days at 25°C. The clear zone around sample disks was measured as the growth inhibition diameter of algae [11].

3. Results and Discussion

Resultant blends formed by varying the amounts of PEG and SS were characterized by different spectroscopic techniques, and their antifouling potential was ascertaining by antialgal assay.

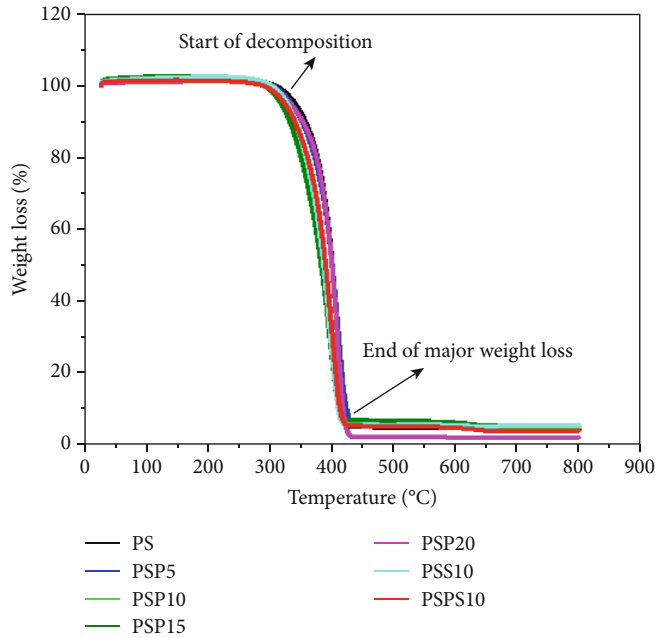

Figure 3: TGA thermographs of the polymer blend samples.

Table 2: Decomposition temperature (T_d) and melting temperature (T_m) of blends (PS, PSP5-20, PSS10, and PSPS10).

Samples	T_d	T_m
PS	350.3	441.2
PSP5	316.9	431.2
PSP10	315.6	428.5
PSP15	313.4	426.7
PSP20	310.5	425.3
PSS10	335.4	434.1
PSPS10	330.5	432.2

3.1. FTIR Spectroscopy of Blends. Various functional groups in the synthesized blends were identified by the FTIR spectroscopy (Figure 2). In the PSS10 blend, the absorption bands at 3060 cm^{-1} and 3026 cm^{-1} were due to aromatic C-H stretching vibrations. Three absorption signals at the wave numbers 1600 cm^{-1}, 1492 cm^{-1}, and 1452 cm^{-1} were due to aromatic C=C stretching vibrations which has indicated the presence of benzene ring [20]. The absorptions at the 756 cm^{-1} and 698 cm^{-1} were corresponded to C-H out-of-plane bending vibrations. This has indicated that there was only one substituent in the benzene ring [21]. SS has exhibited characteristic signals at 1125 cm^{-1} for SO_2 and at 1655 cm^{-1} for NH_2 group which has confirmed the successful blend formation. The IR spectrum of PSP10 blend has shown stretching vibrations of –OH groups at 3463 cm^{-1} and C-O at 1645 cm^{-1} for polymeric part corresponding to PEG [22]. In the PSPS10 blend, signatures of all functional group were detected like C=C stretching vibrations of PS at 1452 cm^{-1}, C-O and -OH signals of PEG at 1645 cm^{-1} and 3463 cm^{-1}, and NH_2 and SO_2 bands of SS at 1655 cm^{-1} and 1125 cm^{-1}, respectively, as shown in Figure 2.

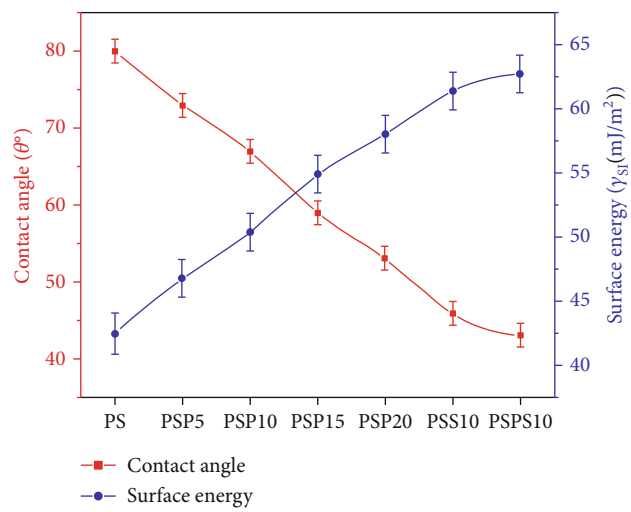

Figure 4: Blend composition and water contact angles.

3.2. Thermal Stability. Thermogravimetric analysis (TGA) was performed to determine the thermal stability of polymeric blends [21]. The TGA curves of various polymer blend samples are depicted in Figure 3. The basic thermogravimetric trend corresponding to various samples was almost identical. Thermal decomposition was started in the range of 310°C to 350°C as given in Table 2. The major structural decomposition occurred between 350°C and 420°C with the negligible amount of decomposition and continued till 800°C. Blending has affected the thermal stability of PS which depends upon the amount of PEG incorporated into blends, although it tends to decrease the thermal stability of polystyrene blends but not more than 25°C at any decomposition stage [21]. PEG is relatively a low-melting polymer in comparison with polystyrene that has reduced the thermal stability of corresponding blends while the initial

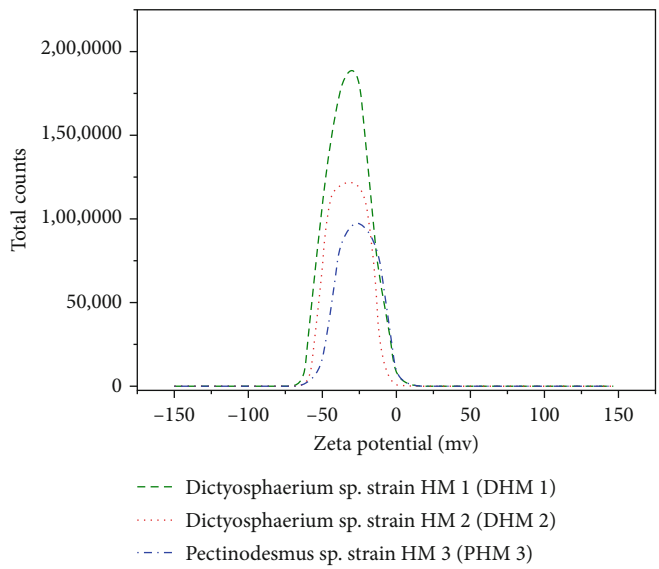

Figure 5: Zeta Potential of algal strains DHM1, DHM2, and DHM3.

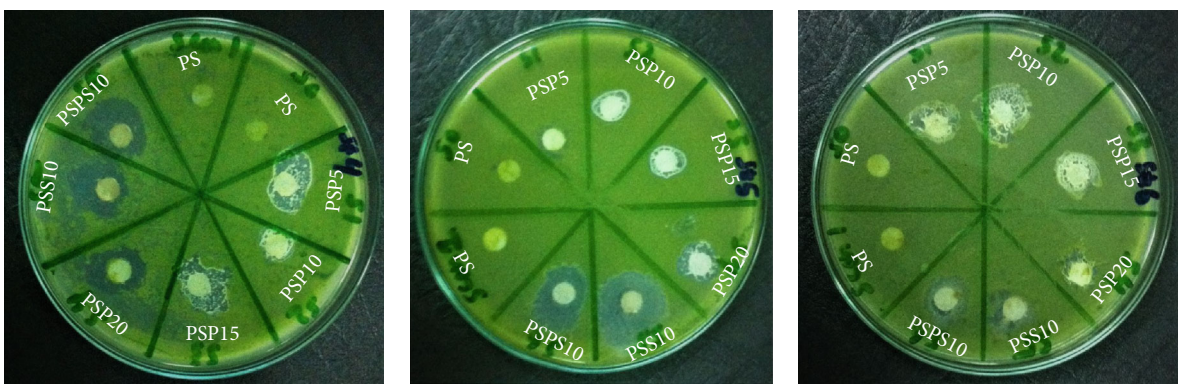

(a) (b) (c)

Figure 6: Microalgae-cultured plates with the disk diffusion method against (a) *Dictyosphaerium* sp., strain HM1 (DHM1), (b) *Dictyosphaerium* sp., strain HM2 (DHM2), and (c) *Pectinodesmus* sp., strain HM3 (PHM3).

decomposition temperature of blends remains high in comparison with room temperature where most of the polymers are practically used [21].

Contrary to PEG, SS has improved the thermal stability of PSS10 polymer blends to a notable extent. Ternary blend PSPS10 tends to decompose by few degrees earlier when compared with binary PSS10 blends in most of the cases due to PEG. All polymeric blends were found thermally stable even at 300°C [23, 24].

3.3. Contact Angle and Surface Energy. Hydrophilicity of various polymer blends was measured in terms of contact angle as shown in Figure 4. The static contact angle of virgin PS was found to be 80°, and increasing the concentration of PEG, the contact angle was decreased [25]. The PSP5 blend with 5% PEG concentration has demonstrated contact angle of 66° [26]. By increasing the concentration of PEG up to 10% in the PSP10 blend, the contact angle was found to be 63° [27]. The PSP15 and PSP20 blends with 15% and 20% concentration of PEG shown to have the contact angles of 65° and 53°, respectively [27]. Since PEG is hydrophilic in nature due to the presence of hydroxyl group, therefore by increasing the PEG contents, it has increased hydrophilicity of the blends which has resulted in the decrease of water contact angle [28, 29].

Further addition of 10% silver sulfadiazine (SS) in the PSS10 blend has increased the hydrophilicity due to the polar nature of SS and decreased the contact angle of blend to 46° [22]. The polarity of SS has caused more strong attraction of water molecules on blend's surface [30]. The PSPS10 blend with 10% SS and 10% PEG concentration has shown the lowest contact angle, i.e., 43°. The decrease in the contact angle of PSPS10 is due to presence of hydroxyl group in PEG and polarity of SS that tends to increase the hydrophilic nature of PSP10 [31, 32].

Among various blend compositions, the surface energy (γs) of virgin PS has exhibited the minimum surface energy (42 ± 1 mJ/m^2), and its surface energy has increased from 47 to 58 mJ/m^2 upon addition of 5-20% hydrophilic PEG in PS, respectively [33]. Upon addition of SS into PS, it caused

further increased of surface energy up to 61 mJ/m^2 in the PSS10 blend while the PSPS10 ternary blend has exhibited the maximum γs value, i.e., 63 mJ/m^2 [34]. Surface energy and contact angle have inverse relationship as shown in Figure 4. Generally, higher surface energy of material caused more bioadhesion and reduced antialgal activity [35]. But in this study, increase of surface energy did not lead to decrease of antialgal activities. This has indicated that biofilm adhesion is not a major antialgal factor in these blended materials.

3.4. Zeta Potential and Size of Algal Strains. Zeta potential and surface charges are important features that determine surface properties like hydrophilicity, hydrophobicity, and bioadhesion [36, 37]. Zeta potential values of *Dictyosphaerium* sp. (DHM1), *Dictyosphaerium* sp. (DHM2), and *Pectinodesmus* sp. (PHM3) algal strains were found to be -32.7 mV, -33.0 mV, and -25.7 mV, respectively (Figure 5) [38], whereas the average diameter of algal strains was measured as 179.6 nm, 102.6 nm, and 70.4 nm corresponding to *Dictyosphaerium* sp. (DHM1), *Dictyosphaerium* sp. (DHM2), and *Pectinodesmus* sp. (PHM3), respectively. There was no discernible difference in the zeta potential of different algae strains. Therefore, all the strains have exhibited almost identical behavior against different polymer blends. Microbial organisms are negatively charged over a wide pH range [39]. Zeta potential leads to electrostatic interaction that results in the adhesion of microorganisms on surfaces; thus, fouling may increase with the increase in zeta potential [40].

3.5. Antialgal Activity. The inhibition of algal growth by polymer blends was quantitatively measured in terms of inhibition zone diameter [11]. The inhibition zones of polymer blends against *Dictyosphaerium* sp. (DHM1), *Dictyosphaerium* sp. (DHM2), and *Dictyosphaerium* sp. (DHM3) are depicted in Figures 6 and 7. The green lawn on agar plates has confirmed algal growth while each tested polymer blend has exhibited particular inhibition zone depending upon its composition and concentration [41]. Results have revealed that PS has demonstrated no inhibition zone thus no antifouling activity. Among various PSP5-20 blends, PSP5 has the lowest PEG, and PSP20 has the highest PEG concentration. From PSP5 to PSP20, the inhibition zone against DHM1 was increased from 8.5 mm to 9.3 mm, against DHM2 from 9.1 mm to 9.3 mm, and against DHM3 from 8.6 mm to 9.7 mm, respectively [42]. This has clearly shown the direct relationship between the amount of hydrophilic PEG in blend and its antialgal properties [43]. The inhibition zone was increased with the addition of SS in PSS10 blend 10.2 mm, 10.2 mm, and 11.4 mm inhibition zone against DHM1, DHM2, and DHM3 algal strains, respectively, as given in Table 3. Most significant antialgal behavior was observed in the PSPS10 blend owing to the presence of both hydrophilic components, i.e., PEG and SS. This has demonstrated the highest zone of inhibition, i.e., 10.5 mm, 10.5 mm, and 11.4 mm against DHM1, DHM2, and DHM3 algal strains, respectively, as depicted in Figures 6 and 7.

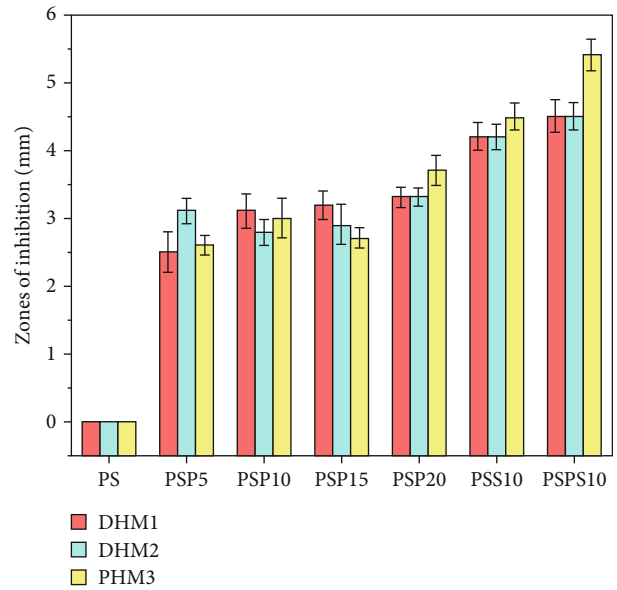

Figure 7: The antialgal analysis of various compositions of blends (PS, PSP5-20, PSS10, and PSPS10) against different algal strains (DHM1, DHM2, and PHM3).

Table 3: Contact angle, surface energy, and zone of inhibition of blends (PS, PSP5-20, PSS10, and PSPS10).

Samples	Contact angle (θ)	Surface energy (γs)	Zone of inhibition (mm)		
			DHM1	DHM2	PHM3
PS	80	42.52	0	0	0
PSP5	73	46.83	8.5	9.1	8.6
PSP10	67	50.42	9.1	8.8	9
PSP15	59	54.92	9.2	8.9	8.7
PSP20	53	58.07	9.3	9.3	9.7
PSS10	46	61.41	10.2	10.2	10.5
PSPS10	43	62.74	10.5	10.5	11.4

The hydrophilicity, high mobility, conformation, neutral charge, and hydrogen bonding capacities of PEG are considered critical in their antifouling efficiency [44]. The hydrophilic character of PEG lowers the interfacial free energy for the water thus weakens the adsorption forces for proteins [45]. When a protein reaches the PEG mount surface, then a limited amount of conformation would be available in the PEG chains due to steric stabilization [46]. The protein will concurrently displace any water connected to PEG units, thus altering the state of water polymer solvation [47]. Both phenomenon, i.e., hydrophilicity and conformation would boost the system's free energy, so the mechanism would not be conducive, and the protein would retain away from the surface [47, 48]. The high mobility of PEG chains would shorten the protein interaction time on the surface, thereby minimizing the adsorbed volumes [49]. Moreover, hydrogen bonding of water molecules across the PEG chains produces some sort of bound water shell structure that serves to deter proteins from approaching [50, 51].

Incorporation of SS to blends PSS10 and PSPS10 resulted in even higher algal growth inhibition in comparison with PSP5-20. The amino group present in SS has enhanced the antialgal activity of materials because it increased the hydrophilic nature of blends [52]. Owing to the hydrophilicity of SS, hydration shells of water are formed on the blend surface that repels algal strains [53]. The ternary blend PSPS10 was proved to be the best prepared composition that resulted in the maximum algal growth inhibition of 10.5 mm for DHM1, 10.5 mm for DMH2, and 11.4 mm for PHM3 due to the presence of strong antifouling agent silver sulfadiazine and PEG.

4. Conclusions

The antialgal synergistic potential of polystyrene blends with polyethylene glycol and silver sulfadiazine is revealed in this work. Results have concluded that both antialgal agents, i.e., PEG and SS, have worked synergistically in polystyrene matrix to improve the antialgal potential as evident from a direct relationship between the amount of antialgal agent and its inhibition zones against microbial growth. All prepared compositions of PSP, PSS, and PSPS blends were proved quite effective against algal species *Dictyosphaerium* sp. (DHM1), *Dictyosphaerium* sp. (DHM2), and *Pectinodesmus* sp. (PHM3) while the ternary blend PSPS10 was the most effective one due to the cooccurrence of both antialgal agents and exhibited maximum zone of inhibitions against all algal strains. Contact angle and surface energy values have highlighted that bioadhesion is not a limiting factor in the fouling of these prepared blends. Thermographs obtained from TGA have demonstrated the thermal stability of blends while a zetasizer has measured the significant values of zeta potential and particle size. These significant results about thermal stability and antialgal features of prepared polystyrene/polyethylene glycol/silver sulfadiazine blends have widen their scope in the fields of marine coatings.

Data Availability

The data used to support the findings of this study is included within the article.

Conflicts of Interest

The authors declare no conflict of interest.

Acknowledgments

All authors are grateful to the NUST Research Directorate for financial assistance. Dr. Nasir M. Ahmad acknowledge HEC, NRPU through Project No. 3526 and 6020, for financial support.

References

[1] C. C. C. R. de Carvalho, "Marine biofilms: a successful microbial strategy with economic implications," *Frontiers in Marine Science*, vol. 5, pp. 1–11, 2018.

[2] G. D. Bixler and B. Bhushan, "Biofouling: lessons from nature," in *Philosophical Transactions of the Royal Society A: Mathematical, Physical and Engineering Sciences*, vol. 370, no. 1967, 2012.

[3] A. S. Carlini, L. Adamiak, and N. C. Gianneschi, "Biosynthetic Polymers as Functional Materials," *Macromolecules*, vol. 49, no. 12, pp. 4379–4394, 2016.

[4] M. Salta, J. A. Wharton, P. Stoodley et al., "Designing biomimetic antifouling surfaces," *Philosophical Transactions of the Royal Society A: Mathematical, Physical and Engineering Sciences*, vol. 368, pp. 4729–4754, 2010.

[5] M. Cobos, I. De-La-Pinta, G. Quindós, M. J. Fernández, and M. D. Fernández, "Synthesis, physical, mechanical and antibacterial properties of nanocomposites based on poly (vinyl alcohol)/graphene oxide–silver nanoparticles," *Polymers*, vol. 12, pp. 1–18, 2020.

[6] Z. Qiao, D. Xu, Y. Yao, S. Song, M. Yin, and J. Luo, "Synthesis and antifouling activities of fluorinated polyurethanes," *Polymer International*, vol. 68, pp. 1361–1366, 2019.

[7] S. Aishwarya, J. Shanthi, and R. Swathi, "Surface energy calculation using Hamaker's constant for polymer/silane hydrophobic thin films," *Materials Letters*, vol. 253, pp. 409–411, 2019.

[8] A. M. C. Maan, A. H. Hofman, W. M. de Vos, and M. Kamperman, "Recent developments and practical feasibility of polymer-based antifouling coatings," *Advanced Functional Materials*, vol. 30, 2020.

[9] B. Ran, C. Jing, C. Yang, X. Li, and Y. Li, "Synthesis of efficient bacterial adhesion-resistant coatings by one-step polydopamine-assisted deposition of branched polyethylenimine-g-poly(sulfobetaine methacrylate) copolymers," *Applied Surface Science*, vol. 450, pp. 77–84, 2018.

[10] A. Krywko-Cendrowska, S. di Leone, M. Bina, S. Yorulmaz-Avsar, C. G. Palivan, and W. Meier, "Recent advances in hybrid biomimetic polymer-based films: from assembly to applications," *Polymers*, vol. 12, 2020.

[11] A. Gitchaiwat, A. Kositchaiyong, K. Sombatsompop, B. Prapagdee, K. Isarangkura, and N. Sombatsompop, "Assessment and characterization of antifungal and antialgal performances for biocide-enhanced linear low-density polyethylene," *Journal of Applied Polymer Science*, vol. 128, pp. 371–379, 2013.

[12] W. Yandi, S. Mieszkin, M. E. Callow et al., "Antialgal activity of poly(2-(dimethylamino)ethyl methacrylate) (PDMAEMA) brushes against the marine alga Ulva," *Biofouling*, vol. 33, pp. 169–183, 2017.

[13] R. B. Bodkhe, S. J. Stafslien, J. Daniels et al., "Zwitterionic siloxane-polyurethane fouling-release coatings," *Progress in Organic Coatings*, vol. 78, 2014.

[14] S. Mushtaq, N. M. Ahmad, H. Nasir, A. Mahmood, and H. A. Janjua, "Transpicuous-cum-fouling resistant copolymers of 3-sulfopropyl methacrylate and methyl methacrylate for optronics applications in aquatic medium and healthcare," *Advances in Polymer Technology*, vol. 2020, 11 pages, 2020.

[15] J. S. Suk, Q. Xu, N. Kim, J. Hanes, and L. M. Ensign, "PEGylation as a strategy for improving nanoparticle-based drug and gene delivery," *Advanced Drug Delivery Reviews*, vol. 99, pp. 28–51, 2016.

[16] J. Wu, W. Lin, Z. Wang, S. Chen, and Y. Chang, "Investigation of the hydration of nonfouling material poly(sulfobetaine methacrylate) by low-field nuclear magnetic resonance," *Langmuir*, vol. 28, pp. 7436–7441, 2012.

[17] B. K. D. Ngo and M. A. Grunlan, "Protein resistant polymeric biomaterials," *ACS Macro Letters*, vol. 6, pp. 992–1000, 2017.

[18] S. R. Meyers and M. W. Grinstaff, "Biocompatible and bioactive surface modifications for prolonged in vivo efficacy," *Chemical Reviews*, vol. 112, pp. 1615–1632, 2012.

[19] S. Newport, B. Differ, K. Hoelzer et al., "Agar disk diffusion and automated microbroth dilution produce similar antimicrobial susceptibility testing results," *Foodborne pathogens and disease*, vol. 8, 2011.

[20] F. Junfei, X. Yimin, and L. I. Qiang, "Preparation of polystyrene spheres in different particle sizes and assembly of the PS colloidal crystals," *Science China Technological Sciences*, vol. 53, pp. 3088–3093, 2010.

[21] A. Sari, C. Alkan, and A. Biçer, "Synthesis and thermal properties of polystyrene-graft-PEG copolymers as new kinds of solid-solid phase change materials for thermal energy storage," *Materials Chemistry and Physics*, vol. 133, pp. 87–94, 2012.

[22] X. Liu, H. Gan, C. Hu et al., "Silver sulfadiazine nanosuspension-loaded thermosensitive hydrogel as a topical antibacterial agent," *International Journal of Nanomedicine*, vol. 14, pp. 289–300, 2019.

[23] H. Bley, B. Fussnegger, and R. Bodmeier, "Characterization and stability of solid dispersions based on PEG/polymer blends," *International Journal of Pharmaceutics*, vol. 390, pp. 165–173, 2010.

[24] F. H. Falqi, O. A. Bin-Dahman, M. Hussain, and M. A. Al-Harthi, "Preparation of Miscible PVA/PEG Blends and Effect of Graphene Concentration on Thermal, Crystallization, Morphological, and Mechanical Properties of PVA/PEG (10 wt%) Blend," *International Journal of Polymer Science*, vol. 2018, 10 pages, 2018.

[25] G. Lin, X. Zhang, S. R. Kumar, and J. E. Mark, "Improved hydrophilicity from poly(ethylene glycol) in amphiphilic conetworks with poly(dimethylsiloxane)," *Silicon*, vol. 1, pp. 173–181, 2009.

[26] M. Inutsuka, H. Tanoue, N. L. Yamada, K. Ito, and H. Yokoyama, "Dynamic contact angle on a reconstructive polymer surface by segregation," *RSC Advances*, vol. 7, pp. 17202–17207, 2017.

[27] L. Li, S. Liu, R. Liu, C. Geng, and Z. Hu, "Preparation and characterization of hydrophilic wetting-modified polyamide fibers," *Advances in Polymer Technology*, vol. 2020, 7 pages, 2020.

[28] Y. Ma, F. Shi, J. Ma, M. Wu, J. Zhang, and C. Gao, "Effect of PEG additive on the morphology and performance of polysulfone ultrafiltration membranes," *Desalination*, vol. 272, pp. 51–58, 2011.

[29] M. A. Abbas, S. Mushtaq, W. A. Cheema et al., "Surface Modification of TFC-PA RO Membrane by Grafting Hydrophilic pH Switchable Poly(Acrylic Acid) Brushes," *Advances in Polymer Technology*, vol. 2020, 12 pages, 2020.

[30] H. Razavi, M. H. Darvishi, and S. Janfaza, "Silver sulfadiazine encapsulated in lipid-based nanocarriers for burn treatment," *Journal of Burn Care & Research*, vol. 39, pp. 319–325, 2018.

[31] P. Kim, D. H. Kim, B. Kim et al., "Fabrication of nanostructures of polyethylene glycol for applications to protein adsorption and cell adhesion," *Nanotechnology*, vol. 16, pp. 2420–2426, 2005.

[32] A. Taglietti, G. Dacarro, D. Barbieri et al., "High bactericidal self-assembled nano-monolayer of silver sulfadiazine on hydroxylated material surfaces," *Materials*, vol. 12, 2019.

[33] Y. C. Chao, S. K. Su, Y. W. Lin, W. T. Hsu, and K. S. Huang, "Interfacial properties of polyethylene glycol/vinyltriethoxysilane (PEG/VTES) copolymers and their application to stain resistance," *Journal of Surfactants and Detergents*, vol. 15, pp. 299–305, 2012.

[34] M. Venkataraman and M. Nagarsenker, "Silver sulfadiazine nanosystems for burn therapy," *AAPS PharmSciTech*, vol. 14, pp. 254–264, 2013.

[35] C. A. Del Grosso, C. Leng, K. Zhang et al., "Surface hydration for antifouling and bio-adhesion," *Chemical Science*, vol. 11, no. 38, pp. 10367–10377, 2020.

[36] J. A. Finlay, M. E. Callow, L. K. Ista, G. P. Lopez, and J. A. Callow, "The influence of surface wettability on the adhesion strength of settled spores of the green alga Enteromorpha and the diatom amphora," *Integrative and Comparative Biology*, vol. 42, pp. 1116–1122, 2002.

[37] F. Hejda, P. Sola˘, and J. Kousal, "Surface free energy determination by contact angle measurements – a comparison of various approaches," *WDS'10*, pp. 25–30, 2010.

[38] M. Khalid, N. Khalid, I. Ahmed, R. Hanif, M. Ismail, and H. A. Janjua, "Comparative studies of three novel freshwater microalgae strains for synthesis of silver nanoparticles: insights of characterization, antibacterial, cytotoxicity and antiviral activities," *Journal of Applied Phycology*, vol. 29, pp. 1851–1863, 2017.

[39] W. F. Walkenhorst, J. W. Klein, P. Vo, and W. C. Wimley, "PH dependence of microbe sterilization by cationic antimicrobial peptides," *Antimicrobial Agents and Chemotherapy*, vol. 57, pp. 3312–3320, 2013.

[40] O. Nedela, P. Slepicka, and V. Švorcík, "Surface modification of polymer substrates for biomedical applications," *Materials*, vol. 10, no. 10, p. 1115, 2017.

[41] D. Debalke, M. Birhan, A. Kinubeh, and M. Yayeh, "Assessments of antibacterial effects of aqueous-ethanolic extracts of Sida rhombifolia's aerial part," *Scientific World Journal*, vol. 2018, pp. 1–8, 2018.

[42] K. M. Dobosz, C. A. Kuo-Leblanc, T. Emrick, and J. D. Schiffman, "Antifouling ultrafiltration membranes with retained pore size by controlled deposition of Zwitterionic polymers and poly(ethylene glycol)," *Langmuir*, vol. 35, pp. 1872–1881, 2019.

[43] T. Ekblad, G. Bergström, T. Ederth et al., "Poly(ethylene glycol)-containing hydrogel surfaces for antifouling applications in marine and freshwater environments," *Biomacromolecules*, vol. 9, no. 10, pp. 2775–2783, 2008.

[44] S. Chen, L. Li, C. Zhao, and J. Zheng, "Surface hydration: principles and applications toward low-fouling/nonfouling biomaterials," *Polymer*, vol. 51, pp. 5283–5293, 2010.

[45] C. Sanchez-Cano and M. Carril, "Recent developments in the design of non-biofouling coatings for nanoparticles and surfaces," *International Journal of Molecular Sciences*, vol. 21, pp. 1–24, 2020.

[46] P. B. Lawrence and J. L. Price, "How PEGylation influences protein conformational stability," *Current Opinion in Chemical Biology*, vol. 34, pp. 88–94, 2016.

[47] L. Guerrini, R. A. Alvarez-Puebla, and N. Pazos-Perez, "Surface modifications of nanoparticles for stability in biological fluids," *Materials*, vol. 11, pp. 1–28, 2018.

[48] K. Terpiłowski, "Apparent surface free energy of polymer/paper composite material treated by air plasma," *International Journal of Polymer Science*, vol. 2017, 8 pages, 2017.

[49] A. Larsson, T. Ekblad, O. Andersson, and B. Liedberg, "Photografted poly(ethylene glycol) matrix for affinity interaction studies," *Biomacromolecules*, vol. 8, pp. 287–295, 2007.

[50] C. Q. Sun, "Aqueous charge injection: solvation bonding dynamics, molecular nonbond interactions, and extraordinary solute capabilities," *International Reviews in Physical Chemistry*, vol. 37, pp. 363–558, 2018.

[51] A. C. Noguer, S. Kiil, and S. Hvilsted, "Long-Term Stability of PEG-Based Antifouling Surfaces in a Marine Environment," in *12th Coatings Science International Conference 2016*, Noordwijk, Netherlands, 2016.

[52] T. Dai, Y.-Y. Huang, K. S. Sharma, T. J. Hashmi, B. D. Kurup, and R. M. Hamblin, "Topical antimicrobials for burn wound infections," *Recent patents on anti-infective drug discovery*, vol. 5, no. 2, pp. 124–151, 2010.

[53] I. Francolini, C. Vuotto, A. Piozzi, and G. Donelli, "Antifouling and antimicrobial biomaterials: an overview," *Apmis*, vol. 125, pp. 392–417, 2017.

Hindawi
Advances in Polymer Technology
Volume 2020, Article ID 5392074, 11 pages
https://doi.org/10.1155/2020/5392074

Research Article

Transpicuous-Cum-Fouling Resistant Copolymers of 3-Sulfopropyl Methacrylate and Methyl Methacrylate for Optronics Applications in Aquatic Medium and Healthcare

Shehla Mushtaq,[1] Nasir M. Ahmad,[2] Habib Nasir,[1] Azhar Mahmood,[1] and Hussnain A. Janjua[3]

[1]*Department of Chemistry, School of Natural Sciences (SNS), National University of Sciences and Technology, H-12, Islamabad 44000, Pakistan*
[2]*Polymer Research Group, School of Chemical and Materials Engineering (SCME), National University of Sciences and Technology, H-12, Islamabad 44000, Pakistan*
[3]*Department of Industrial Biotechnology, Atta-Ur-Rahman School of Applied Biosciences (ASAB), National University of Sciences and Technology, H-12, Islamabad 44000, Pakistan*

Correspondence should be addressed to Nasir M. Ahmad; nasir.ahmad@scme.nust.edu.pk

Received 10 July 2020; Accepted 10 September 2020; Published 5 October 2020

Academic Editor: Alexandra Mu oz Bonilla

The scope of optical sensors and scanners in aquatic media, fluids, and medical diagnostics has been limited by paucity of transparent shielding materials with antifouling potential. In this research endeavor, facile synthesis, characterization, and bioassay of antifouling transparent functional copolymers are reported. Copolymers of 3-sulfopropyl methacrylate (SPMA) and methyl methacrylate (MMA) were synthesized by free radical polymerization in various proportions. Samples PSM20, PSM30, PSM40, PSM50, and PSM60 contain 20%, 30%, 40%, 50%, and 60% SPMA by weight, respectively. Resultant products were characterized by FTIR and ^{1}H-NMR spectroscopy. The synthesized copolymers have exhibited excellent transparency, i.e., 75% to 88%, as determined by the UV-Vis spectroscopic analysis. Transmittance was decreased from 6% to 2% in these copolymers upon changing the concentration of 3-sulfopropyl methacrylate from 20% to 50% owing to bacterial and algal biofilm formation. Water contact angle values were ranged from 18° to 63° and decreased with the increase in the polarity of copolymers. The surface energy lowest value 58 mJ/m^2 and highest value 72 mJ/m^2 were calculated for PSM20 and PSM50, respectively, by the Chibowski approach and Young equation. Sample PSM50 has exhibited the highest antibacterial activities, i.e., 18 mm and 19 mm, against *Escherichia coli* and *Staphylococcus aureus*, respectively, by the disk diffusion method. Copolymer PSM50 has shown minimum algal adhesion for *Dictyosphaerium* algae as observed by optical microscopy. This lower bacterial and algal adhesion is attributed to higher concentrations of anionic SPMA monomer that cause electrostatic repulsion between functional groups of the polymer and microorganisms. Thus, the resultant PSM50 product has exhibited good potential for optronics shielding application in aquatic medium and medical diagnostics.

1. Introduction

Biofouling is an undesirable growth of different types of microorganisms at a material surface that causes various problems including deterioration of polymeric materials, corrosion of metals, and decline in equipment efficiency [1]. Biofouling also damaged input/output signals of sensors and scanners installed in aquatic bodies by increasing opacity of transparent shields. Polymers are synthesized with specific functional groups to combat biofilm formation for a number of applications [2, 3]. Antifouling copolymer with a defined ratio between hydrophobic and hydrophilic monomer units is a facile approach to control microbial growth at a commercial scale [4, 5]. In the field of polymers, two fundamental kinds of materials can be recognized, contingent upon whether the additive is temporarily enclosed within the

polymer or permanently connected with the chains [6, 7]. Advances in polymerization techniques have facilitated the development of more complex polymer structures some of which have been investigated as synthetic antifouling polymers [8, 9]. So far, most of the research has been focused on customizing the composition of copolymer systems, where chemical functionalities are disseminated over the length of a polymer chain [10, 11]. Antifouling polymers are emerging materials for biocidal applications in several critical areas where surface contacts may risk being attacked by bacteria, viruses, and algae [12]. For instance, around 80–95% of hospital-acquired urinary tract infections originate from urinary catheters [13]. This is even more relevant now taking into account the ongoing COVID-19 situation, where materials and surfaces are susceptible to attachment of harmful species, and thus indicates the importance of the transparent antifouling polymers in healthcare applications. These antifouling polymeric products are broadly used in medical devices, packaging products, and delivery systems for solid and liquid pharmaceuticals [12]. Various techniques have been used for the synthesis of antifouling polymers; among them, free radical polymerization provides a specific approach for modification of polymer and its subsequent applications [14]. Free radical polymerization is a vital technique for the synthesis of macromolecules and consistent with a wide range of functional groups, which are not compatible with metal-catalyzed and ionic polymerization [15]. It is initiated by using several initiators like ammonium persulfate, potassium persulfate, and azobisisobutyronitrile [16]. The most significant and vital factor is the precise temperature range of 20-100°C to proceed free radical polymerization in a highly controlled manner as compared to other polymerization techniques due to its exothermic nature [17]. Free radical polymerization is not affected by protic impurities like water and can be performed in bulk [18]. Acrylic monomers are readily synthesized due to ester functional groups and produce a number of polymers with different characteristics [19, 20]. Former analysis has proposed that these properties of the hydration layer on polymeric chains are very critical to assess the origin of the repulsing force against protein and have significant effects on the degree of protein adsorption [21, 22]. This strong hydration effect leads to strong resistance against fouling organisms [22]. Adherence of fouling organisms is the initial step leading to biofilm formation that reduces the efficiency of the materials with time and causes significant limitations to the endpoint utility of many materials [23]. Monomers with a sulfonated functional group have been reported in a number of biocidal applications through different synthetic approaches such as copolymerization and grafting [3]. Many studies have been taken in this regard among which Ahmed et al., which have done grafting of poly-3-sulfopropyl methacrylate (PSPMA) onto carboxymethyl cellulose (CMC) via free radical polymerization technique, have reported 3.1 ± 1.2 antibacterial activity [24]. Oh et al. synthesized brushes of SPMA negatively charged monomers with positively charged and neutral acrylate monomers for deadhesion of bacteria 28 ± 9 nN·nm [25]. Mai et al. have synthesized copolymers of SPMA and polyethylene oxide (PEO) to study biofilm inhibition on teeth [26, 27]. In previous studies, surface modification and incorporation of nanoparticles were done using 3-sulfopropyl methacrylate monomer, and antifouling properties were studied but not primarily focused on their transparency.

In consideration of the challenges and significance of transparency along with antifouling characteristics, herein, novel copolymers were synthesized by optimizing their transparency and antifouling property. Transparent antifouling copolymers of 3-sulfopropyl methacrylate (SPMA) and methyl methacrylate (MMA) are synthesized by free radical polymerization in the presence of water along with DMF as solvent by changing monomer ratios in copolymers. Antifouling effects and percent transmittance of copolymers were studied by changing compositions of SPMA and MMA monomers as presented in Scheme 1. These copolymers with a low water contact angle and high surface energy have shown good antifouling activity against Gram +/-ve bacteria and microalgae (*Dictyosphaerium species*). Antibacterial activity against *E. coli* and *S. aureus* has been probed by the disk diffusion method, and further bacterial biofilm has been analyzed by SEM [28]. Algal biofilm for *Dictyosphaerium species* has been examined by optical microscopy [29]. The results of the current work are significant and provide a facile approach to develop functional antifouling polymers by optimizing transparency for potential applications in various areas including healthcare.

2. Materials and Methods

2.1. Materials. All chemicals were of analytical grade and utilized without any further purification or additional treatment. Methyl methacrylate (MMA) (Sigma, USA), 3-sulfopropyl methacrylate (SPMA) (Sigma-Aldrich, Germany), azobisisobutyronitrile (AIBN), dimethylformamide (DMF), ethanol, paraformaldehyde (PFA), and NaOH were acquired from Sigma-Aldrich (Germany). Tryptose broth (TSB) (Merck, Germany), phosphate buffer solution (PBS) (Amresco, Belgium), Mueller-Hinton agar (MHA) (Daejung, Korea), and BG11 medium (Scharlau, Spain) were used for algal growth. For the bioassays, *E. coli* (ATTC 8739), *S. aureus* (ATCC 6538), and *Dictyosphaerium* sp. (microalgae) were used as representative strains. All solutions and suspensions were prepared by distilled water.

2.2. Synthesis of Copolymers. Polymerization of acrylate monomers was accomplished through the free radical polymerization technique in DMF and water at 70°C under inert atmosphere by 2,2′-azobisisobutyronitrile (AIBN) as an initiator (Figure 1) [20]. For synthesis of the PSM50 sample, polymerization of SPMA and MMA was performed in DMF : water 60 : 40 (*v*/*v*) medium and with |SPMA|MMA|AIBN| 1 : 1 : 0.002 molar ratios. SPMA (1 g, 4.8 mmol), MMA (1 g, 9.9 mmol), AIBN (0.002 g, 0.0121 mmol), DMF (12 ml), and H_2O (8 ml) were introduced in a three-neck flask. Polymerization was executed under continuous nitrogen gas purging to keep the inert environment in the flask while temperature was maintained at around 70°C through oil bath. After polymerization, solvent was removed by a rotary evaporator and the copolymer was dried in a vacuum

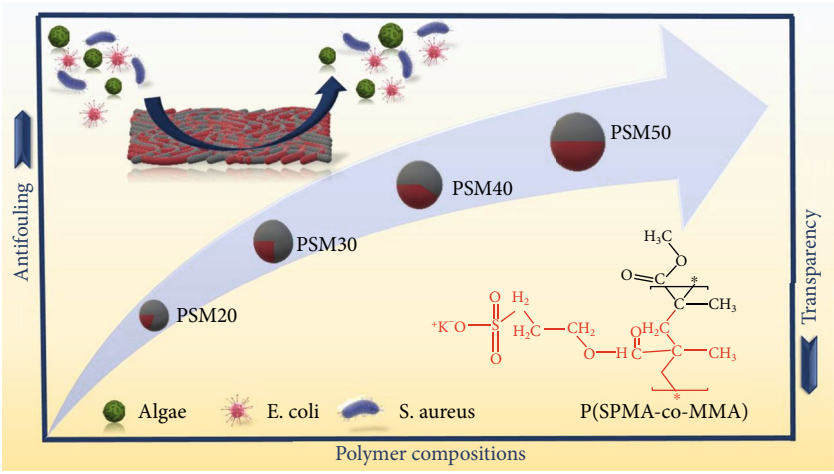

Scheme 1: Overview of synthesized antifouling polymers of P(SPMA-co-MMA) to highlight the influence of antifouling and transparency.

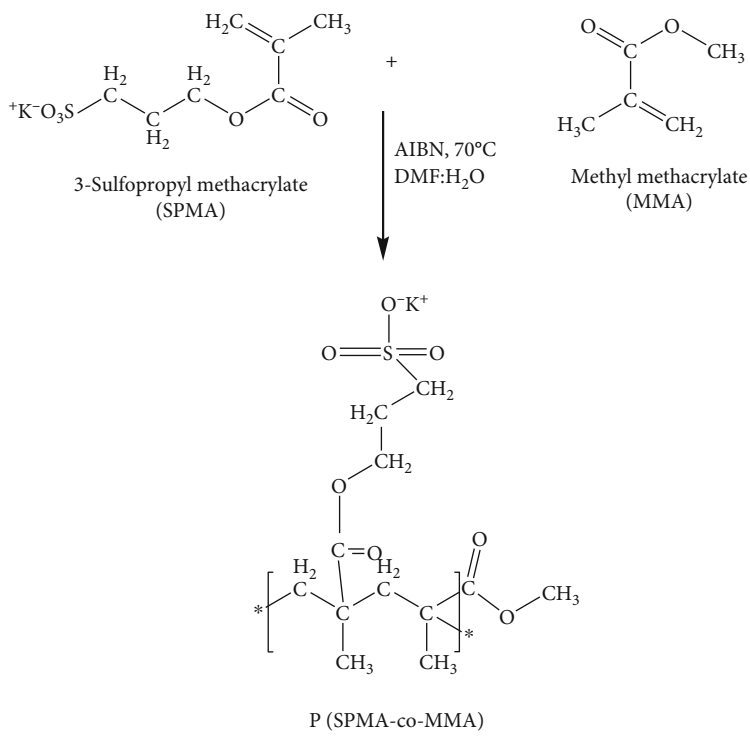

Figure 1: Synthesis of copolymers P(SPMA-co-MMA) through polymerization of 3-sulfopropyl methacrylate (SPMA) and methyl methacrylate (MMA).

oven at 600 mm pressure and 40°C temperature in a petri dish. After drying the copolymer, PSM50 was removed from the petri dish in the form of a transparent sheet. For synthesis of different copolymer samples, the above procedure was repeated except that the concentration of SPMA and MMA monomers was changed as tabulated in Table 1.

2.3. Characterization and Bioassay. Fourier Transform Infrared Spectroscopy (FTIR) was performed using the Bruker, ALPHA-P FTIR spectrometer for functional group determination. ^{1}H-NMR spectra were acquired through the Bruker, ASCEND 400 MHz NMR spectrometer by dissolving 3 mg sample into 1 ml deuterated DMSO solvent at 343 K temperature [30]. UV-Visible spectroscopy was performed on JENWAY7315 to analyze transparency of these copolymers and to calculate absorption maxima (λ_{max}) values due to $\pi - \pi^*$ electronic transition of functional groups from SPMA and MMA monomers [31]. The equilibrium water contact angles of sample size $1 \times 1\,cm^2$ were measured by using the drop analyzer of Kruss DSA 25 at room temperature while advancing and receding angles were computed from the average of at least five measurements [32]. Bacterial and algal adhesions

Table 1: Sample codes with concentration of SPMA and MMA.

Sample codes	Weight (%)		Concentration (mmol)		Mol (%)	
	SPMA	MMA	SPMA	MMA	SPMA	MMA
PSM60	60	40	5.75	7.99	41.85	58.15
PSM50	50	50	5.36	9.98	32.66	67.34
PSM40	40	60	3.83	11.98	24.23	75.77
PSM30	30	70	2.87	13.98	17.032	82.96
PSM20	20	80	1.97	15.98	10.97	89.03

on the surface of polymeric materials were investigated by the JEOL JSM-6490LA scanning electron microscope and OPTIKA 600 optical microscope, respectively.

Antibacterial activity was performed by the disk diffusion method using gentamycin as a negative control and PMMA as a positive control. Bacteria were stored in a lag phase at -4°C in the form of agar plate and activated before antibacterial assay. Bacteria were streaked on a freshly prepared Mueller-Hinton agar (MHA) plate and put into an oven already set at 37°C for 24 hours. Bacterial colony from new growth was mixed into saline, and optical density was set 0.5 by using the McFarland standard after centrifuging. Bacterial cultures (1 ml) of *E. coli* and *S. aureus* were poured on agar. MHA plates were again placed in the oven at 37°C for 24 hours, and the zone of inhibitions was observed [33]. All experiments were performed at least three times, and the results are presented as the mean ± standard deviation. Statistical significance was determined using the *t*-test ($^{*}p < 0.05$, $^{**}p < 0.01$, $^{***}p < 0.001$, and $^{****}p < 0.0001$) [34]. The biofilm formation test was performed for *E. coli*, ATCC 8739, and *S. aureus* ATCC 6538 in six-well plates, and as-prepared copolymers of size 0.5 × 0.5 cm were put into each well for 24 hours. Retrieved samples were further treated with PBS, 4% PFA, and different concentrations of ethanol. Drying was carried out in sterile petri plates to avoid contamination. After drying, samples were placed at -4°C until subjected to SEM analysis [35]. *Dictyosphaerium* microalgae were employed for biofilm formation testing. Inocula of *Dictyosphaerium* were taken from freshly grown medium of optimum light and air. These cells were centrifuged and washed with distilled water. The optical density was set at 0.5 for the spectrophotometer [29]. The adhesion studies were carried out using *Dictyosphaerium* on prepared antifouling copolymers P(SPMA-co-MMA), and comparative analysis was made by using each type of copolymer. The inoculum was prepared from the stock cultures by aptly reducing their concentration with BG11 to acquire 1.0×10^7 cell/ml suspension. Each sample of size $1 \times 1\,cm^2$ was placed in a glass-sterilized petri dish, and algal suspension was poured on top of the copolymers. These petri plates were centrifuged at 40 rpm under 85 ± 10 $\mu mol\,m^{-2}\,S^{-1}$ of illumination. After a period of 7 days, polymeric samples were recovered from the plates and thoroughly washed with distilled water. Fixation of algal cells was further proceeded by washing copolymers with 2.5% glutaraldehyde, 0.1 M phosphate buffer, and different concentrations of ethanol, respectively. Optical microscopy was used to check algal adhesion on copolymers P(SPMA-co-MMA) [29].

3. Results and Discussion

3.1. FTIR Analysis. Various prepared samples of PSPMA, PMMA, and P(SPMA-co-MMA) were analyzed by FTIR spectroscopy to study their functional groups in Figure 2. In the FTIR spectrum of PSPMA, the band at 2960 cm^{-1} was due to C–H asymmetric stretching vibration [36] while absorption at 2897 cm^{-1} was assigned to C–H symmetric stretching vibration [37]. C=O stretching vibration was depicted at 1726 cm^{-1} [37], and the band at 1450 cm^{-1} was attributed to saturated ester [38]. This spectrum has shown C–H asymmetric deformation of CH_3 at 1485 cm^{-1} and C –H symmetric deformation of CH_3 at 1475 cm^{-1} [30]. The signals at 1190 cm^{-1} and 1041 cm^{-1} were assigned to symmetric stretching vibration and asymmetric stretching vibration of the SO_3 group [30]. In the FTIR spectrum of PMMA, the band at 1433 cm^{-1} was assigned to the asymmetric bending vibration of the CH_3 group of PMMA [39]. The absorption value at 1381 cm^{-1} was due to OCH_3 deformation of PMMA [39]. The characteristic signals observed at 1265 cm^{-1} and 1145 cm^{-1} correspond to C–O–C stretching and bending, respectively [39]. The FTIR band at 1193 cm^{-1} was due to –OCH_3 stretching vibration. Vibrations at 977 cm^{-1} and 716 cm^{-1} were assigned to the CH_2 wagging and rocking modes of PMMA, respectively [40].

In the PSM50 spectrum, characteristic bands were observed at 749 cm^{-1} due to stretching of the –CH_2 group of polymer [38]. The FTIR band was obtained at 1041 cm^{-1} due to asymmetric stretching vibration of SO_3 [41]. The bands due to -C-O stretching vibration of esters were read at 1354 cm^{-1} and 1145 cm^{-1} [19]. In the FTIR spectra of PSPMA, PMMA, and P(SPMA-co-MMA), no absorption was observed for C=C bond in the 1610-1680 cm^{-1} range; this has confirmed that polymerization was taking place at the vinyl group due to which C=C double bond signals disappeared [37].

3.2. ^{1}H-NMR Spectroscopy. The ^{1}H-NMR spectrum of P(SPMA-co-MMA) copolymer's PSM50 sample in Figure 3 has illustrated that the different chemical shift peaks in DMSO at 343 K corresponded to various proton environments in different chemical moieties present in copolymer [39]. Signals of MMA and SPMA are well observed in the spectrum. There are notable variations in the dynamic motion of protons that validate the structure of copolymer and as a result of association phenomena which depicted eloquent spectral changes [42]. In this spectrum, a standard prominent peak due to DMSO solvent was observed at 2.5 ppm [43]. Another characteristic peak due to the OCH_2 group of SPMA was observed slightly upward at 4.2 ppm [42]. Furthermore, a signal was read at 2.72 ppm due to CH_2SO_3K resonance [42]. The inset showed resonance at 3.1-3.5 ppm which also has indicated the formation of copolymer [43]. The peaks at 1.1 ppm and 1.8 ppm have represented methyl groups along the chains that are surrounded by different environments [38].

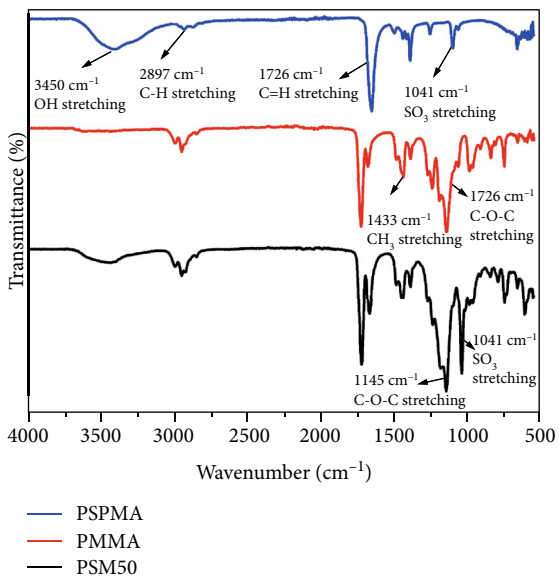

Figure 2: FTIR spectra of as-synthesized samples: poly-3-sulfopropyl methacrylate (PSPMA), polymethylmethacrylate (PMMA), and PSM50 copolymer of P(SPMA-co-MMA).

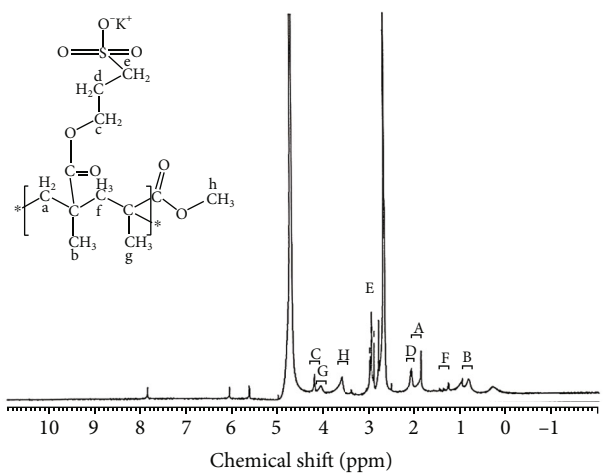

Figure 3: ^{1}H-NMR of PSM50 copolymer of P(SPMA-co-MMA).

3.3. UV-Vis Spectroscopy. UV-Vis spectra in Figure 4 of P(SPMA-co-MMA) copolymers have shown absorbance in the range of 200-320 nm wavelength. It is evident from spectra that PSM20 and PSM30 have greater transmittance ≈88% and ≈85% as compared to PSM40 and PSM50 that have ≈81% and ≈76%, respectively. Copolymers PSM50 and PSM40 have shown intense absorbance below 300 nm as compared to PSM30 and PSM20. This absorption edge was generated due to the electronic excitation within the sulfonyl group (O=S=O) and carbonyl group (C=O) chromophores present in copolymers [38]. The most intense absorption band detected in the spectra from 200 to 250 nm is due to $\pi - \pi^*$ transition in the O=S=O and C=O systems [44].

Figure 4 has also depicted the transmittance as a function of incident light wavelength while transmittance decreased and absorbance increased with increasing the concentration

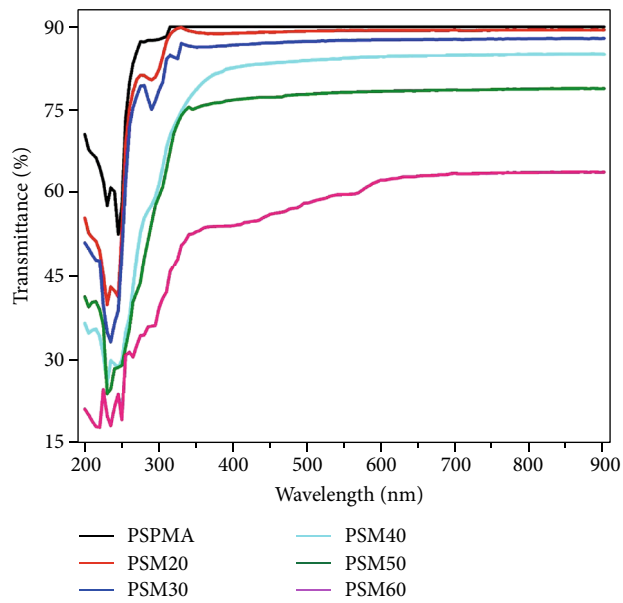

Figure 4: UV-Visible spectra of the synthesized copolymers of poly-3-sulfopropyl methacrylate and methyl methacrylate, P(SPMA-co-MMA).

of SPMA monomer in copolymers PSM20 to PSM60. However, transmittance of PSM60 was significantly decreased upon increasing SPMA concentration which resulted in loss of transparency. This is due to the presence of free electrons in SPMA that absorb the electromagnetic energy of the incident light and excited to higher energy levels to occupy energy bands that caused less light penetration through it [45]. As concluded from Figure 4, transparency of PSM60 was quite low so it was insignificant for further characterization and application. On the other hand, the MMA monomer has high transmittance because MMA has no free electrons that move towards the conduction band on photon absorption [45].

Transparency of these copolymers was affected after biofilm formation as shown in Figure 5. PSM50 has greater concentration of SPMA monomer and is expected to possess higher antifouling property due to hydrophilic negatively charged sulfonated groups. Copolymers with more SPMA monomer resulted in minimal adhesion of microorganisms and low biofilm that lead to small decrease in percent transmittance. In PSM50, concentration of SPMA monomer was 50%, and 2% decrease in transmittance was observed after biofilm formation while in PSM20 concentration of SPMA monomer was 20% resulting in more adhesion of fouling organisms; thus, 6% decrease in transmittance was observed after biofilm formation. Copolymers PSM40 and PSM30 with 40% and 30% of SPMA monomer contents by weight exhibited transmittance between PSM50 and PSM20 with 3 ± 2% transmittance decrease after biofilm formation.

3.4. Contact Angle and Surface Energy Measurement. Contact angles of the synthesized copolymers P(SPMA-co-MMA) were observed to be highly dependent on the molar ratio of SPMA monomer in Figure 6. Copolymers PSM50, PSM40,

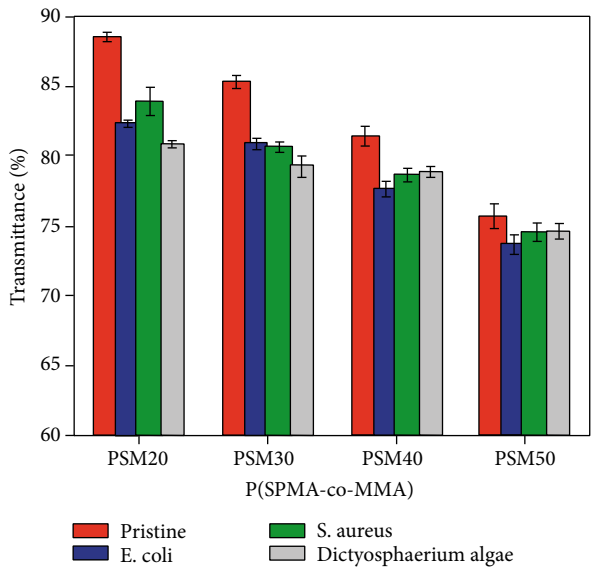

Figure 5: %Transmittance comparison of copolymers of P(SPMA-co-MMA); before (pristine) and after biofilm formation against *E. coli*, *S. aureus*, and *Dictyosphaerium* algae.

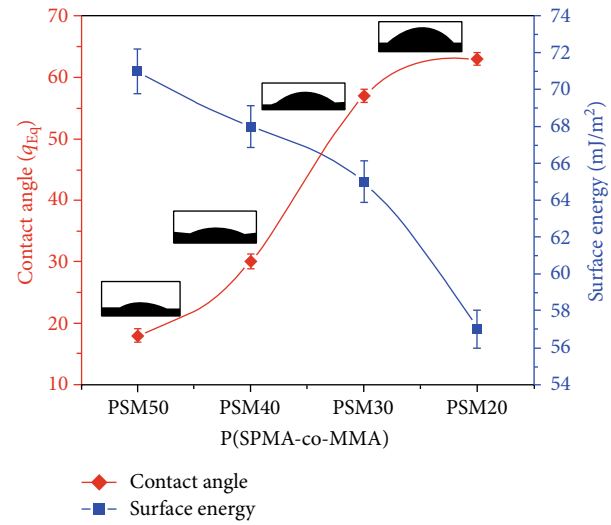

Figure 6: Contact angles and surface energy of the prepared copolymers of P(SPMA-co-MMA).

PSM30, and PSM20 have demonstrated contact angles 17°, 29°, 56°, and 63°, respectively. The water contact angle is notably influenced by the interactions of polar liquid, e.g., water with hydrophilic functional groups of P(SPMA-co-MMA) copolymer like the SO_3 group [46]. At the water-polymer interface, there are polar water molecule interactions and orientation with anionic functional groups of polymer structural chain [46]. Water molecules on a polymer chain can be directed away from the solid-gas interface after changing their orientation [37]. The apparent surface free energy was also estimated based on the equilibrium water contact angle approach [47]. Surface energy is increased with the decrease in the equilibrium water contact angles as clearly reflected in Figure 6 [46]. The calculated surface free energy values are dependent upon the physicochemical properties of the water [48]. Chibowski correlation, Young equation, and the equilibrium contact angle were applied for the computation of apparent surface free energy [46, 49]:

$$\gamma_s = \frac{\gamma_l}{2}\left(1 + \cos\ \theta_{Eq}\right), \tag{1}$$

where γ_s is the apparent surface free energy, γ_l is the liquid surface tension, and θ_{Eq} is the equilibrium contact angle.

3.5. Antibacterial Activity. The antibacterial activity of copolymers P(SPMA-co-MMA) with various concentrations of SPMA was performed against Gram-positive bacteria *S. aureus* and Gram-negative bacteria *E. coli* by the disk diffusion method while measurements were recorded in terms of inhibition zones. Figures 7(a) and 7(b) represent the evaluation of antifouling activity of the copolymers compared with a drug (gentamycin) as a positive control and PMMA as a negative control, respectively. It was observed that synthesized copolymers have significant antibacterial activity against *E. coli* and *S. aureus*. The statistical analysis of copolymers was performed using the paired two-tailed *t*-test technique by establishing the mean and standard deviation of an individual copolymer. Error bars show the standard deviation, and asterisks (∗) represent significant *p* values.

It was observed that antibacterial activity was enhanced by increasing concentration of anionic SPMA hydrophilic monomer in the synthesized copolymers P(SPMA-co-MMA) [50]. Bacterial settlement and adhesion are primarily dependent upon surface roughness, hydrophobicity, hydrophilicity, and electrostatic charges present on the material surfaces [25, 51]. In these synthesized copolymers, the anionic sulfonated group produced electrostatic repulsive forces on the material surface [37, 42]. These electrostatic repulsive forces played a vital role in forming significant inhibition zones with the increase of the SPMA monomer contents [43]. The bacterial cell wall is made up of macromolecules comprising carboxylate, phosphate, and amino functional groups that induced electrostatic charge to the cell periphery [52]. Both bacteria *S. aureus* and *E. coli* have a negative charge on the outer surface due to phospholipids in the structure and repelled by the copolymers containing anionic SO_3 groups in SPMA monomer due to repulsive electrostatic interactions [53]. These results suggested that higher concentrations of SPMA monomer in the copolymer compositions may have produced more repulsion between polymer and bacteria [35, 54]. This increase in SPMA monomer concentration in copolymers resulted in enhanced water hydrogen bonding and lower fouling [21]. These anionic copolymers are capable of effectively interacting with water molecules that resulted in lower settlement of bacteria to higher extent [35].

3.6. SEM Analysis of Bacterial Biofilm. Biofilm formation on the surface of prepared copolymers was also studied by SEM technique in Figures 8 and 9. Biofilm development, composition, distribution, and substratum relationships are well investigated by SEM technique in literature [55–57].

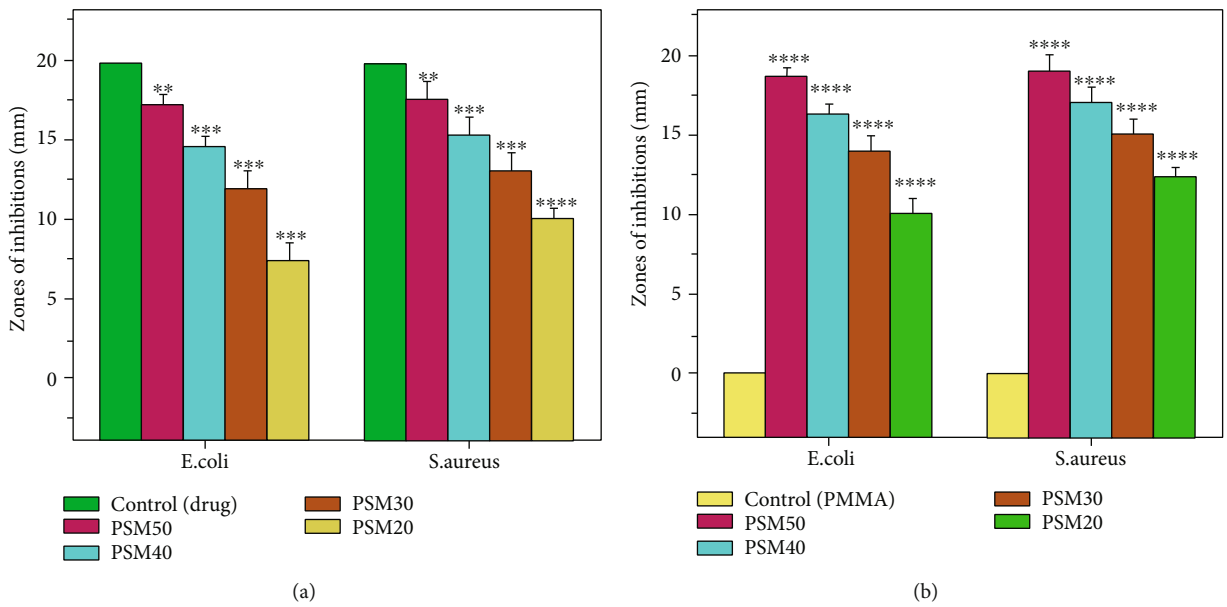

Figure 7: Zones of inhibition of PSM50, PSM40, PSM30, and PSM20 for *E. coli* and *S. aureus*: (a) with drug (+ive control) and (b) with PMMA (-ive control).

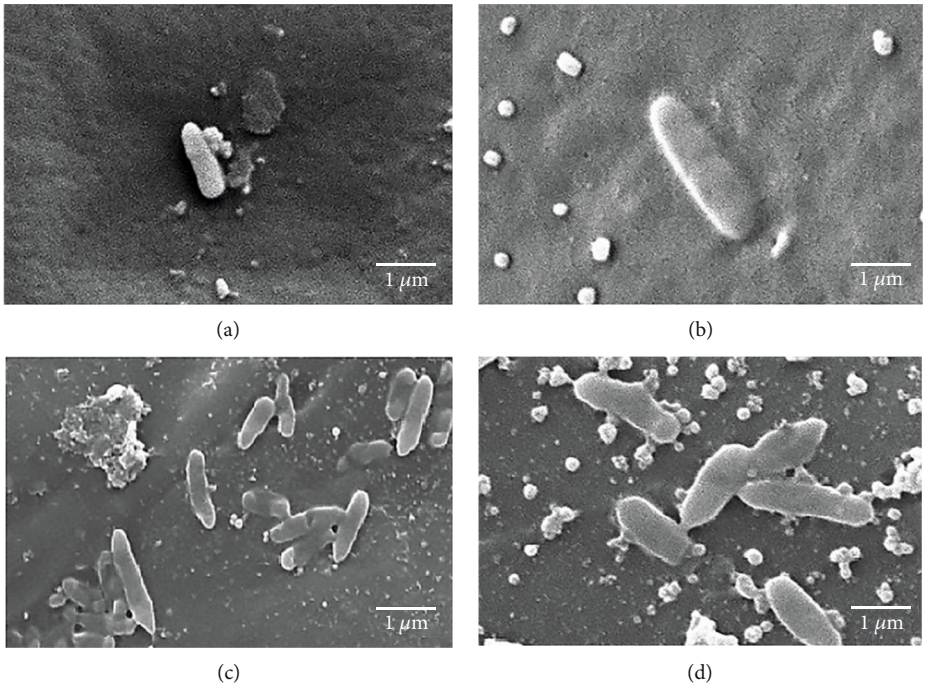

Figure 8: SEM images of *E. coli* biofilm adhesion on (a) PSM50, (b) PSM40, (c) PSM30, and (d) PSM20.

As evident, the synthesized copolymers exhibited excellent antibacterial activity against *E. coli* and *S. aureus*. Adhesion of these bacteria was reduced on synthesized copolymer due to electrostatic repulsion as a result of identical negative charges on materials and bacterial surface [58]. In these copolymers, sulfonated groups of SPMA monomer have been increased from PSM20 to PSM50 by 20-50 wt% that enhanced hydration and lower pH which apply stress on the outer membrane of these tested bacteria by exerting pressure on the bacterial cell wall [59]. SEM images have also shown low adhesion of *E. coli* and *S. aureus* on the surface due to the hydrophilic and anionic nature of SPMA monomer [49, 51]. The bacteria motility is expected to diminish on negatively charged polymers and resulted in protein denaturation, enzyme denaturation, and microbial death by rupturing the cell wall of Gram-negative bacteria *E. coli* and Gram-positive bacteria *S. aureus* [35, 53, 60]. In Figures 8 and 9, adhesion of *E. coli* and *S. aureus* on the surface of

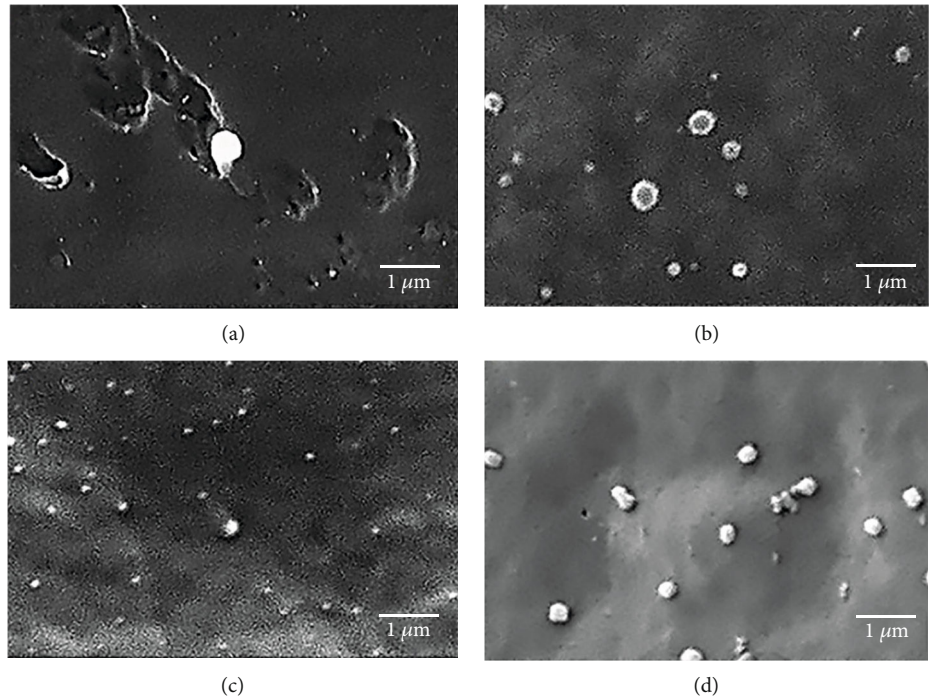

Figure 9: SEM images of *S. aureus* biofilm adhesion on (a) PSM50, (b) PSM40, (c) PSM30, and (d) PSM20.

PSM50 and PSM40 was low due to greater content of SPMA monomer as compared to PSM30 and PSM20 with less content of anionic SPMA monomer. This biofilm formation and adhesion were controlled by electrostatic repulsion between bacteria and surface of material [5, 61]. On the other hand, rupturing of the bacterial cell wall was also observed in SEM images of *E. coli* in Figures 8(a) and 8(c) and *S. aureus* in Figures 9(a) and 9(b) due to charged polymers and protein denaturation.

3.7. Optical Microscopy of Algal Biofilm. Optical microscopic images of algal biofilm on prepared copolymer surfaces are presented in Figure 10. Results have shown lower adhesion of *Dictyosphaerium* algae on PSM50 and PSM40 due to higher concentration of SPMA monomer in the synthesized copolymers. Adhesion of algae depends on multiple factors like material chemical nature, charge on algae, and surface free energy [21]. These parameters measure the ability of a surface to interlink with other materials by interactions that highly depend on interfacial surface energies [21]. The hydrophilic nature of SPMA monomer leads to the hydration layer on the surface of material that resulted in low algal biofilm formation on the surface [62]. Higher concentration of SPMA monomer also caused high surface energy thus showing minimum adhesion of algal cells [63].

The adhesions of *Dictyosphaerium* algae on P(SPMA-co-MMA) copolymers were decreased due to electrostatic repulsion that originated as a result of similar negative charges on the cell membrane of *Dictyosphaerium* algae and copolymer [64]. Greater repulsion upon algal species *Dictyosphaerium* and minimum algal adhesion on surface were demonstrated in PSM50 and PSM40 due to higher negatively charged content of SPMA monomer as compared to PSM30 and PSM20 [64].

4. Conclusion

P(SPMA-co-MMA) copolymers were successfully synthesized by free radical polymerization with varying wt% of methyl methacrylate (MMA) and 3-sulfopropyl methacrylate (SPMA) monomers. These copolymer samples PSM50, PSM40, PSM30, and PSM20 were transparent while percent transmittance was increased by increasing MMA contents from 50% (PSM50) to 80% (PSM20). However, copolymer sample PSM60 has lost transparency owing to low contents of MMA, i.e., 40%. Water contact angle values of copolymers were varied from 20° to 65° by varying contents of hydrophilic SPMA monomer and hydrophobic MMA monomer. Surface energy of the synthesized copolymers ranged from 57 mJ/m^2 to 70 mJ/m^2. These copolymers have exhibited good antifouling activity against bacteria *E. coli* and *S. aureus* and against microalgae *Dictyosphaerium*. The transparent antifouling polymers have shown low bacterial and algal biofilm formation with increasing content of SPMA monomer due to electrostatic repulsion between bacteria and polymers. SEM images showed rupturing of the bacterial cell wall due to hydration and decrease in pH which enhanced pressure on the outer membrane of bacteria. After biofilm formation, a slight decrease in transparency was observed around 2-8% of copolymer samples due to the difference in adhesion capacity of microorganisms on different hydrophilic materials. Algal biofilm of *Dictyosphaerium* sp. has exhibited a low adhesion level owing to electrostatic repulsion between microalgae and anionic copolymers. PSM50 had more

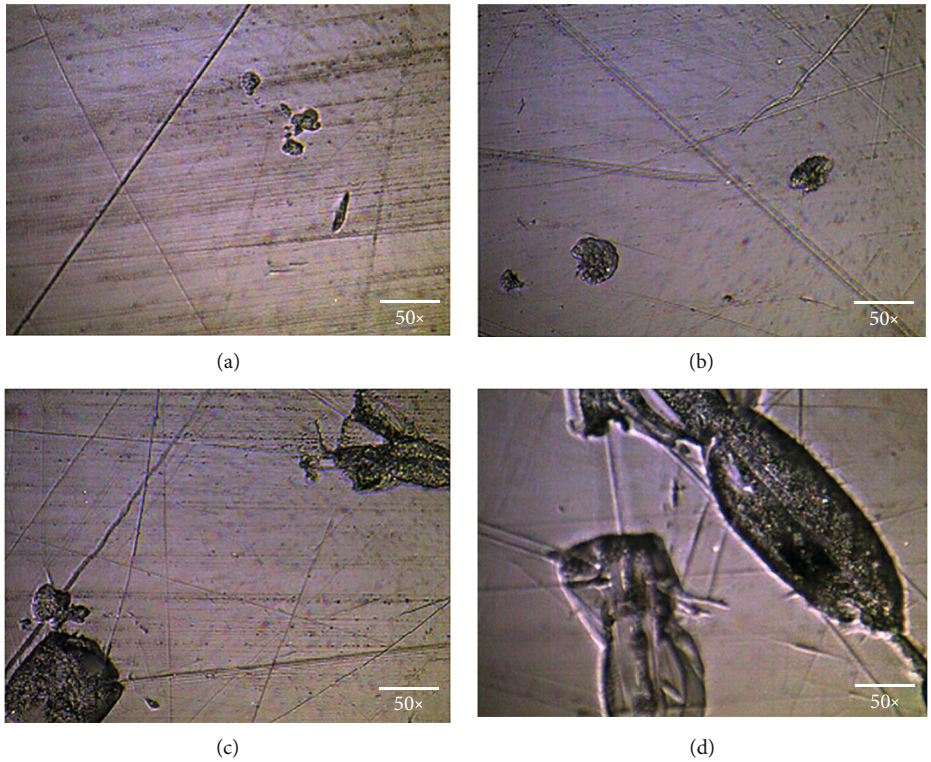

Figure 10: Optical microscopy of algal biofilm of *Dictyosphaerium* for the various copolymers of P(SPMA-co-MMA): (a) PSM50, (b) PSM40, (c) PSM30, and (d) PSM20.

hydrophilicity and greater negatively charged sulfonated group of SPMA monomer that lead to more repulsion and low settlement of algae on the polymer surfaces. These tailor-designed P(SPMA-co-MMA) copolymers have exhibited significantly higher transparency and inhibit biofilm formation on the surface that make them promising candidate materials for various applications including optronics in aquatic media, healthcare, and biotechnology.

Data Availability

The data used to support the findings of this study is included within the article.

Conflicts of Interest

The authors declare no conflict of interest.

Acknowledgments

The authors are grateful to the National University of Sciences and Technology Research Directorate for financial support. Dr. Nasir M. Ahmad acknowledges the support of HEC, NRPU, through Project No. 3526.

References

[1] C. Wu, Y. Zhou, H. Wang, J. Hu, and X. Wang, "Formation of antifouling functional coating from deposition of a zwitterionic-co-nonionic polymer via "grafting to" approach," *Journal of Saudi Chemical Society*, vol. 23, no. 8, pp. 1080–1089, 2019.

[2] A. Alamri, M. H. el-Newehy, and S. S. al-Deyab, "Biocidal polymers : synthesis and antimicrobial properties of benzaldehyde derivatives immobilized onto amine-terminated polyacrylonitrile," *Chemistry Central Journal*, vol. 6, no. 1, p. 1, 2012.

[3] L. Timofeeva and N. Kleshcheva, "Antimicrobial polymers: mechanism of action, factors of activity, and applications," *Applied Microbiology and Biotechnology*, vol. 89, no. 3, pp. 475–492, 2011.

[4] J. Baggerman, M. M. J. Smulders, and H. Zuilhof, "Romantic surfaces: a systematic overview of stable, biospecific, and antifouling zwitterionic surfaces," *Langmuir*, vol. 35, no. 5, pp. 1072–1084, 2019.

[5] V. B. Damodaran and N. S. Murthy, "Bio-inspired strategies for designing antifouling biomaterials," *Biomaterials Research*, vol. 20, no. 1, pp. 1–11, 2016.

[6] M. A. Hood, M. Mari, and R. Muñoz-Espí, "Synthetic strategies in the preparation of polymer/inorganic hybrid nanoparticles," *Materials*, vol. 7, no. 5, pp. 4057–4087, 2014.

[7] K. Müller, E. Bugnicourt, M. Latorre et al., "Review on the processing and properties of polymer nanocomposites and nanocoatings and their applications in the packaging, automotive and solar energy fields," *Automotive and Solar Energy Fields*, vol. 7, no. 4, p. 74, 2017.

[8] R. Nugraha, J. A. Finlay, S. Hill et al., "Antifouling properties of oligo (lactose)-based self-assembled monolayers," *Biofouling*, vol. 31, no. 1, pp. 123–134, 2014.

[9] M. Salta, J. A. Wharton, P. Stoodley et al., "Designing biomimetic antifouling surfaces," *Philosophical Transactions of the*

Royal Society A - Mathematical Physical and Engineering Sciences, vol. 368, no. 1929, pp. 4729–4754, 2010.

[10] E. F. Palermo, I. Sovadinova, and K. Kuroda, "Structural determinants of antimicrobial activity and biocompatibility in membrane-disrupting methacrylamide random copolymers," *Biomacromolecules*, vol. 10, no. 11, pp. 3098–3107, 2009.

[11] B. van Bochove and D. W. Grijpma, "Photo-crosslinked synthetic biodegradable polymer networks for biomedical applications," *Journal of Biomaterials Science. Polymer Edition*, vol. 30, no. 2, pp. 77–106, 2019.

[12] H. Palza, "Antimicrobial polymers with metal nanoparticles," *International Journal of Molecular Sciences*, vol. 16, no. 1, pp. 2099–2116, 2015.

[13] L. T. Curtis, "Prevention of hospital-acquired infections: review of non-pharmacological interventions," *The Journal of Hospital Infection*, vol. 69, no. 3, pp. 204–219, 2008.

[14] E. R. Kenawy, S. D. Worley, and R. Broughton, "The chemistry and applications of antimicrobial polymers: a state-of-the-art review," *Biomacromolecules*, vol. 8, no. 5, pp. 1359–1384, 2007.

[15] A. Debuigne, T. Radhakrishnan, and M. K. Georges, "Stable free radical polymerization of acrylates promoted by α-hydroxycarbonyl compounds," *Macromolecules*, vol. 39, no. 16, pp. 5359–5363, 2006.

[16] P. Acrylates, D. Avci, K. Avi, and E. Tu, "Modeling the free radical polymerization of acrylates," *International Journal of Quantum Chemistry*, vol. 103, no. 2, pp. 176–189, 2005.

[17] S. Purser, P. R. Moore, S. Swallow, and V. Gouverneur, "Fluorine in medicinal chemistry," *Chemical Society Reviews*, vol. 37, no. 2, pp. 320–330, 2008.

[18] K. Yamada, T. Nakano, and Y. Okamoto, "Stereospecific free radical polymerization of vinyl esters using fluoroalcohols as solvents," *Macromolecules*, vol. 31, no. 22, pp. 7598–7605, 1998.

[19] H. J. Patel, M. G. Patel, A. K. Patel, K. H. Patel, and R. M. Patel, "Synthesis, characterization and antimicrobial activity of important heterocyclic acrylic copolymers," *eXPRESS Polymer Letters*, vol. 2, no. 10, pp. 727–734, 2008.

[20] M. B. Dolia, U. S. Patel, A. Ray, and R. M. Patel, "Synthesis, characterization and antimicrobial activity of novel acrylic copolymers," *Polymer Journal*, vol. 38, no. 2, pp. 159–170, 2006.

[21] M. A. Bag and L. M. Valenzuela, "Impact of the hydration states of polymers on their hemocompatibility for medical applications: a review," *International Journal of Molecular Sciences*, vol. 18, no. 8, p. 1422, 2017.

[22] J. Wu, W. Lin, Z. Wang, S. Chen, and Y. Chang, "Investigation of the hydration of nonfouling material poly (sulfobetaine methacrylate) by low-field nuclear magnetic resonance," *Langmuir*, vol. 28, no. 19, pp. 7436–7441, 2012.

[23] R. O. Darouiche, "Antimicrobial approaches for preventing infections associated with surgical implants," *Clinical Infectious Diseases*, vol. 36, no. 10, pp. 1284–1289, 2003.

[24] A. R. El-Nahas, M. Lachine, E. Elsawy, A. Mosbah, and H. El-Kappany, "A randomized controlled trial comparing antimicrobial (silver sulfadiazine)-coated ureteral stents with non-coated stents," *Scandinavian Journal of Urology*, vol. 52, no. 1, pp. 76–80, 2018.

[25] Y. J. Oh, E. S. Khan, A. CampoDel, P. Hinterdorfer, and B. Li, "Nanoscale characteristics and antimicrobial properties of (SI-ATRP)-seeded polymer brush surfaces," *ACS Applied Materials & Interfaces*, vol. 11, no. 32, pp. 29312–29319, 2019.

[26] T. Mai, E. Rakhmatullina, K. Bleek et al., "Poly (ethylene oxide)- b -poly(3-sulfopropyl methacrylate) block copolymers for calcium phosphate mineralization and biofilm inhibition," *Biomacromolecules*, vol. 15, no. 11, pp. 3901–3914, 2014.

[27] V. Cepas, Y. López, Y. Gabasa et al., "Inhibition of bacterial and fungal biofilm formation by 675 extracts from microalgae and cyanobacteria," *Antibiotics*, vol. 8, no. 2, p. 77, 2019.

[28] A. Muñoz-Bonilla and M. Fernández-García, "Polymeric materials with antimicrobial activity," *Progress in Polymer Science*, vol. 37, no. 2, pp. 281–339, 2012.

[29] F. Pillet, E. Dague, J. Pe, and I. Ru, "Changes in nanomechanical properties and adhesion dynamics of algal cells during their growth," *Bioelectrochemistry*, vol. 127, pp. 154–162, 2019.

[30] T. Mai, K. Wolski, A. Puciul-Malinowska et al., "Anionic polymer brushes for biomimetic calcium phosphate mineralization — a surface with application potential in biomaterials," *Polymers*, vol. 10, no. 10, p. 1165, 2018.

[31] T. Kaino, "Optical Absorption of Polymers," in *Encyclopedia of Polymeric Nanomaterials*, S. Kobayashi and K. Müllen, Eds., Springer, Berlin, Heidelberg, 2014.

[32] D. P. Subedi, "Contact angle measurement for the surface characterization of solids," *Himalayan Physics*, vol. 2, pp. 1–4, 2011.

[33] K. Hoelzer, K. J. Cummings, L. D. Warnick et al., "Agar disk diffusion and automated microbroth dilution produce similar antimicrobial susceptibility testing results for *Salmonella* serotypes Newport, Typhimurium, and 4,5,12:i-, but differ in economic cost," *Foodborne Pathogens and Disease*, vol. 8, no. 12, pp. 1281–1288, 2011.

[34] Y. Wang, Y. Lu, J. Zhang et al., "A synergistic antibacterial effect between terbium ions and reduced graphene oxide in a poly(vinyl alcohol)–alginate hydrogel for treating infected chronic wounds," *Journal of Materials Chemistry B*, vol. 7, no. 4, pp. 538–547, 2019.

[35] B. Ran, C. Jing, C. Yang, X. Li, and Y. Li, "Synthesis of efficient bacterial adhesion-resistant coatings by one-step polydopamine-assisted deposition of branched polyethylenimine-g-poly (sulfobetaine methacrylate) copolymers," *Applied Surface Science*, vol. 450, pp. 77–84, 2018.

[36] J. Gu, S. Yuan, W. Shu, W. Jiang, S. Tang, B. Liang et al., "PVBC microspheres tethered with poly(3-sulfopropyl methacrylate) brushes for effective removal of Pb(II) ions from aqueous solution," *Colloids Surfaces A Physicochem Eng Asp*, vol. 498, pp. 218–230, 2016.

[37] R. Patel, W. S. Chi, S. H. Ahn, C. H. Park, H. K. Lee, and J. H. Kim, "Synthesis of poly (vinyl chloride)-g-poly(3-sulfopropyl methacrylate) graft copolymers and their use in pressure retarded osmosis (PRO) membranes," *Chemical Engineering Journal*, vol. 247, pp. 1–8, 2014.

[38] M. Degirmenci, "Synthesis and characterization of novel well-defined end-functional macrophotoinitiator of poly(MMA) by ATRP," *Journal of Macromolecular Science, Part A*, vol. 42, no. 1, pp. 21–30, 2005.

[39] Shen, "Preparation and characterization of PMMA and its derivative via RAFT technique in the presence of disulfide as a source of chain transfer agent," *Journal of Membrane and Separation Technology*, pp. 117–128, 2012.

[40] C. Park, E. Y. Jung, H. J. Jang, G. T. Bae, B. Shin, and H. S. Tae, "Synthesis and properties of plasma-polymerized methyl methacrylate via the atmospheric pressure plasma polymerization technique," *Polymers*, vol. 11, no. 3, p. 396, 2019.

[41] T. Turhan, Y. G. Avcıbası, and N. Sahiner, "Versatile p(3-sulfopropyl methacrylate) hydrogel reactor for the preparation of Co, Ni nanoparticles and their use in hydrogen production," *Journal of Industrial and Engineering Chemistry*, vol. 19, no. 4, pp. 1218–1225, 2013.

[42] G. Masci, D. Bontempo, N. Tiso et al., "Atom transfer radical polymerization of potassium 3-sulfopropyl methacrylate: direct synthesis of amphiphilic block copolymers with methyl methacrylate," *Macromolecules*, vol. 37, no. 12, pp. 4464–4473, 2004.

[43] Y. Xu, A. Walther, and A. H. E. Müller, "Direct synthesis of poly(potassium 3-sulfopropyl methacrylate) cylindrical polymer brushes via ATRP using a supramolecular complex with crown ether," *Macromolecular Rapid Communications*, vol. 31, no. 16, pp. 1462–1466, 2010.

[44] N. Boens, L. Wang, V. Leen et al., "8-HaloBODIPYs and Their 8-(C, N, O, S) substituted analogues: Solvent dependent UV-Vis spectroscopy, variable temperature NMR, crystal structure determination, and quantum chemical calculations," *The Journal of Physical Chemistry A*, vol. 118, pp. 1576–1594, 2014.

[45] H. N. Najeeb, A. A. Balakit, G. A. Wahab, and A. K. Kodeary, "Study of the optical properties of poly (methyl methacrylate) (PMMA) doped with a new diarylethen compound," *Academic Research International*, vol. 5, pp. 48–56, 2014.

[46] K. Terpiłowski, "Apparent surface free energy of polymer/paper composite material treated by air plasma," *International Journal of Polymer Science*, vol. 2017, 8 pages, 2017.

[47] C. Rulison, "Measure surface energy: a tutorial designed to provide basic understanding of the concept of solid surface energy," Krus USA, 1999.

[48] T. S. Parreidt and M. Schmid, "Validation of a novel technique and evaluation of the surface free energy of food," *Foods*, vol. 6, no. 4, p. 31, 2017.

[49] J. A. Callow, M. E. Callow, L. K. Ista, G. Lopez, and M. K. Chaudhury, "The influence of surface energy on the wetting behaviour of the spore adhesive of the marine alga *Ulva linza* (synonym *Enteromorpha linza*)," *Journal of The Royal Society Interface*, vol. 2, no. 4, pp. 319–325, 2005.

[50] M. Ramstedt, N. Cheng, O. Azzaroni, D. Mossialos, H. J. Mathieu, and W. T. S. Huck, "Synthesis and characterization of poly (3-sulfopropylmethacrylate) brushes for potential antibacterial applications," *Langmuir*, vol. 23, no. 6, pp. 3314–3321, 2007.

[51] J. A. Finlay, M. E. Callow, L. K. Ista, G. P. Lopez, and J. A. Callow, "The influence of surface wettability on the adhesion strength of settled spores of the green alga Enteromorpha and the diatom Amphora," *Integrative and Comparative Biology*, vol. 42, no. 6, pp. 1116–1122, 2002.

[52] L. A. B. Rawlinson, S. M. Ryan, G. Mantovani, J. A. Syrett, D. M. Haddleton, and D. J. Brayden, "Antibacterial effects of poly (2-(dimethylamino ethyl)methacrylate) against selected gram-positive and gram-negative bacteria," *Biomacromolecules*, vol. 11, no. 2, pp. 443–453, 2010.

[53] J. S. Dickson and M. Koohmaraie, "Cell surface charge characteristics and their relationship to bacterial attachment to meat surfaces," *Applied and Environmental Microbiology*, vol. 55, no. 4, pp. 832–836, 1989.

[54] O. Rzhepishevska, S. Hakobyan, R. Ruhal, J. Gautrot, D. Barbero, and M. Ramstedt, "The surface charge of anti-bacterial coatings alters motility and biofilm architecture," *Biomater Sci*, vol. 1, pp. 589–602, 2013.

[55] M. E. Callow and R. L. Fletcher, "The influence of low surface energy materials on bioadhesion - a review," *International Biodeterioration and Biodegradation*, vol. 34, no. 3-4, pp. 333–348, 1994.

[56] Y. Cheng, G. Feng, and C. I. Moraru, "Micro- and nanotopography sensitive bacterial attachment mechanisms: a review," *Frontiers in Microbiology*, vol. 10, 2019.

[57] G. A. James, L. Boegli, J. Hancock, L. Bowersock, A. Parker, and B. M. Kinney, "Bacterial adhesion and biofilm formation on textured breast implant shell materials," *Aesthetic Plastic Surgery*, vol. 43, no. 2, pp. 490–497, 2019.

[58] B. T. Benkhaled, S. Hadiouch, H. Olleik et al., "Elaboration of antimicrobial polymeric materials by dispersion of well-defined amphiphilic methacrylic SG1-based copolymers," *Polymer Chemistry*, vol. 9, no. 22, pp. 3127–3141, 2018.

[59] B. K. D. Ngo and M. A. Grunlan, "Protein resistant polymeric biomaterials," *ACS Macro Letters*, vol. 6, no. 9, pp. 992–1000, 2017.

[60] A. Terada, K. Okuyama, M. Nishikawa, S. Tsuneda, and M. Hosomi, "The effect of surface charge property on Escherichia coli initial adhesion and subsequent biofilm formation," *Biotechnology and Bioengineering*, vol. 109, no. 7, pp. 1745–1754, 2012.

[61] S. Krishnan, J. Weinman, and C. K. Ober, "Advances in polymers for anti-biofouling surfaces," *Journal of Materials Chemistry*, vol. 18, no. 29, pp. 3405–3413, 2008.

[62] A. S. Carlini, L. Adamiak, and N. C. Gianneschi, "Biosynthetic polymers as functional materials," *Macromolecules*, vol. 49, no. 12, pp. 4379–4394, 2016.

[63] D. Park, J. A. Finlay, R. J. Ward et al., "Antimicrobial behavior of semifluorinated-quaternized triblock copolymers against airborne and marine microorganisms," *ACS Applied Materials & Interfaces*, vol. 2, no. 3, pp. 703–711, 2010.

[64] R. Henderson, S. A. Parsons, and B. Jefferson, "The impact of algal properties and pre-oxidation on solid–liquid separation of algae," *Water Research*, vol. 42, no. 8-9, pp. 1827–1845, 2008.